SPECIAL ISSUE ARTICLE





Recent advances in modeling structure-property relations in biomimetic materials at the molecular and continuum scales

Stuti Devendra Upadhyay | Param Punj Singh | Vinay Thakur Raghavan Ranganathan ⁽¹⁾

Department of Materials Engineering, Indian Institute of Technology, Gandhinagar, India

Correspondence

Raghavan Ranganathan, Department of Materials Engineering, Indian Institute of Technology, Gandhinagar, Gujarat, India. Email: rraghav@iitgn.ac.in

Funding information

Anusandhan National Research Foundation (ARNF), Grant/Award Number: CRG/2023/005333

Abstract

Biomimetic materials, inspired by nature's evolutionary designs, offer exceptional mechanical properties that have revolutionized the fields of structural resilience, impact resistance, and fracture mitigation. This review provides a comprehensive overview of recent advances in the modeling and simulations of structure-property relationships in key biomimetic systems, including nacre, dactyl club, spider silk, and bone, across the molecular and continuum scales. Emphasis is placed on how these biological archetypes have been translated into synthetic counterparts using computational tools such as molecular dynamics simulations and finite element method, enabling precise investigations into deformation, fracture, and energy dissipation mechanisms under high-strain rate scenarios like ballistic and impact loading conditions. Furthermore, the review explores the growing potential of artificial intelligence and machine learning to accelerate the design, optimization, and discovery of next-generation biomimetic materials with superior mechanical properties. This review highlights the advances that have bridged the gap between biological inspiration and engineering applications, providing direction for future research in high-performance, multifunctional biomimetic materials.

KEYWORDS

bioceramics, composites, layered crystal structures, mechanical properties

1 | INTRODUCTION

The advancement of material science is increasingly propelled by inspiration drawn from the natural world. In recent decades, biomimicry and bioinspiration have become essential approaches for creating advanced materials with tailored properties that not only match but also exceed the performance and sustainability of their counterparts. ^{1–6} Impact-resistant bioinspired materials have attracted considerable attention due to their poten-

tial applications in various high-performance and protective technologies. These natural impact-resistant materials can be classified based on their structural motifs and microstructural characteristics, including sandwich, tubular, layered, gradient, and sutured architectures. Despite their diversity, these materials share common structural attributes, such as a well-defined hierarchical organization, composite nature, controlled porosity, distinct interfaces, and viscoelastic or viscoplastic behavior. Among the broad spectrum of natural materials, those that exhibit

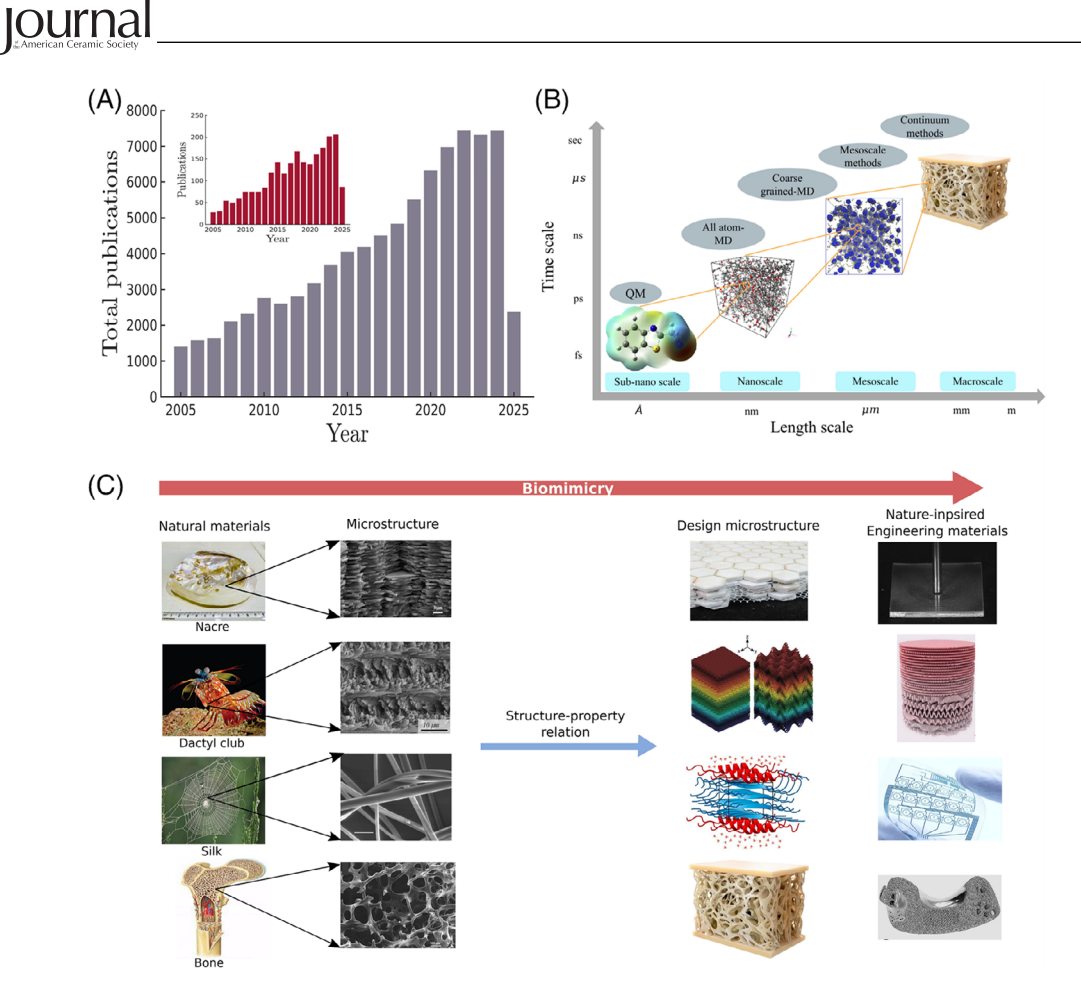


FIGURE 1 (A) Bar plot showing the number of publications on biomimicry of high-performance natural materials compared to the publication trend of computational methods used in biomimicry (inset). Source: Web of Science. (B) Schematic representation of multiscale simulation techniques across numerous length and time scales. (C) Biomimicry of high-performance natural materials in engineering: Examples of nacre, mantis shrimp, silk, and bone showcasing hierarchical microstructures adapted into advanced engineered materials. Source: Reproduced from permissions. 12-16

exceptional impact resistance, such as nacre, bone, dactyl club of the mantis shrimp, and spider silk, have been extensively studied due to their remarkable combination of strength, toughness, resistance to crack propagation, damage, durability, and low density. These superior properties arise from their hierarchical architecture and the synergistic interactions of multiple phases at different length scales, despite being composed of inherently brittle constituents.⁸⁻¹¹ A key challenge is unraveling the fundamental mechanisms that govern the superior properties of these biological composites. Despite extensive efforts to engineer materials with tailored mechanical properties using macroscopic and microscopic design strategies, a comprehensive understanding of the synergistic strengthening and toughening mechanisms occurring across multiple length scales remains elusive but essential for advancing bioinspired materials design.

Over the past couple of decades, there has been a gradual increase in the total number of publications in the field of bioinspired materials, both in computational

and experimental studies, as shown in Figure 1A. The micromechanical behavior of biological and bioinspired materials has been extensively investigated under various loading conditions, including tension, compression, shear, and three-point bending. However, accurate measurement of mechanical properties and elucidation of the underlying mechanisms at the nanoscale using experimental techniques alone remains highly challenging and, in some cases, infeasible. Although techniques such as scanning electron microscopy (SEM) and atomic force microscopy (AFM) provide visualization and quantification of material properties at fine scales, they are constrained by limitations in instrument resolution and sensitivity, as well as challenges in maintaining sample integrity during preparation and testing. As a result, direct experimental validation at the nanoscale remains scarce. To address these limitations, computational modeling, particularly molecular dynamics (MD) simulations, has emerged as a powerful tool for replicating the dynamic behavior of materials at the nanoscale. Additionally, finite element method (FEM) models bridge the nanoscale behavior with bulk material properties, enabling a more comprehensive understanding of structure-property relationships. Figure 1B illustrates the different simulation techniques across the varying length and time scales, including MD and FEM. By integrating experimental observations with theoretical predictions, these computational approaches facilitate the design of next-generation bioinspired materials, offering innovative solutions for diverse engineering applications.

A detailed understanding of the complex structureproperty relationships in these materials is essential for the development of advanced materials with superior impact resistance and multifunctional capabilities. 17,18 These relationships are governed by multiple factors, including microstructure, composition, and intricate interactions across various length scales.¹⁹ The hierarchical architecture of these materials, which incorporates nanoscale reinforcement, microscale toughening mechanisms, and macroscale structural configurations, plays a crucial role in improving impact resistance and mechanical performance. Figure 1C illustrates how nature-inspired materials, such as nacre, mantis shrimp appendages, silk fibers, and bone structures, serve as blueprints for engineering high-performance materials. Each example showcases hierarchical organization, from nanoscale to macroscale, that contributes to exceptional mechanical properties such as toughness, strength, and flexibility. These biological architectures are emulated in synthetic materials to improve performance in fields such as aerospace, biomedicine, and protective systems.

This review highlights recent advances in computational modeling of structure-property relationships in biomimetic materials, covering multiple length scales and employing various computational approaches. Specifically. MD has been instrumental in atomistic-scale simulations, while FEM has provided valuable insights at the continuum level. Using the structural principles of biological systems, researchers are driving the development of advanced bioinspired materials with enhanced mechanical performance. Integrating computational modeling with experimental data and emerging technologies has great potential to address global challenges and meet the growing demand for high-performance materials in diverse engineering applications.^{20,21}

COMPUTATIONAL TECHNIQUES

MD simulations 2.1

MD simulations are useful in predicting the system's thermodynamic, structural, and dynamic properties across a range of length and time scales. MD methods can be

divided into Ab initio MD (AIMD), classical MD, reactive MD, and coarse-grain MD (CGMD). In the AIMD method, the nuclei are still treated as classical particles, and the force acting on them is calculated by solving the Schrödinger equation for the electrons. Although possessing high accuracy, these calculations are computationally very expensive and can only simulate hundreds of atoms. In contrast, the remaining methods employ classical equations of motion to govern atomic behavior, which are time-integrated using well-known algorithms, such as the Leapfrog and Velocity-Verlet methods, 22 with atomic trajectories subsequently recorded over the simulation time. This method can typically simulate a system with millions of atoms with reasonable accuracy. In classical MD, the interaction between particles (typically atoms), also called the force field, is typically divided into bonded and nonbonded interactions. Bonded interactions consider the bond stretching, angular bending, and dihedral (torsional) energy, whereas the nonbonded interactions are defined by Lennard-Jones and electrostatic interactions. It does not involve bond breaking and formation, and helps predict properties where chemical reactions are not involved.

Classical MD simulations are widely applied in fields such as the calculation of diffusivity,²³ mechanical and thermal properties of polymer nanocomposites, ²⁴ protein folding,²⁵ water filtration,²⁶ and so on, to name a few. In contrast, the reactive MD simulations involve potential energy descriptions containing a bond-order-based energy term that can include corrections for over-coordination of bonds, lone-pair interactions, conjugation, and hydrogen bonding.²⁷ The strength of the reactive force fields lies in the accurate description of bond breakage and formation based on the concept of bond orders, and is useful in studying systems where chemical reactions are key parameters in governing the system behavior. Some key applications of reactive MD simulations involve studying electrolyte-electrode interface reaction in battery materials, 28 oxidation of hydrocarbons, 29 thermal decomposition of polymers,³⁰ combustion of fuels,³¹ and so on. Classical and ReaxFF MD represent each atom explicitly, thus making them computationally more demanding. CGMD instead simplifies these systems by grouping several atoms into a single particle, thus reducing the system's degree of freedom and computational complexity. CGMD is routinely used in several fields such as protein folding and aggregation, 32,33 lipid monolayers and bilayers, 34,35 polymers in melt,³⁶ mechanical properties of soft matter systems,^{37,38} metal-organic frameworks,³⁹ and so on. Finally, these simulations provide a robust framework for the detailed understanding and prediction of material behavior at the atomic scale.

In biomimetic material design, classical MD simulations offer insight into the molecular-level interactions

and the complex structural patterns that are responsible for the excellent structural and mechanical properties in biomimetic materials. With increasing computational powers, researchers can simulate larger and complex molecular systems for longer timescales. However, the results of MD methods highly depend on the quality of force fields used. Generally, classical force fields are empirical in nature, whose parameters are derived from experimental observations rather than first-principle calculations. As a result, they suffer from transferability across different systems and accuracy. A detailed discussion on the use of MD in biomimetic materials is presented in the upcoming sections.

2.2 Finite element method

FEM is a powerful numerical analysis technique used to obtain an approximate solution to a class of problems governed by boundary value problems and has been widely used in various branches of science and engineering. The technique was first developed to solve complex mathematical formulations, and was later (around 1950) extended to solve real-world engineering problems in fields such as aeronautical and civil engineering. 40-43 Today, FEM is widely used in biomechanics, 44,45 composite materials, 46 solid mechanics, 47,48 fluid mechanics, 49,50 electromagnetism,⁵¹ heat and mass transfer studies^{52–54} and, in general, in all problems that involve the solution of a partial differential equation. FEM has profoundly transformed scientific modeling and engineering design across a wide array of fields, including automotive, aerospace, aerodynamic flow analysis, nuclear engineering, excavation analysis, bridges, prestressed concrete structures, stress analysis in implants, highway infrastructure, and skyscrapers, to name a few, and played a key role in effective design.

In FEM analysis, the domain or geometry is divided into smaller computational domains or elements (finite elements), each characterized by finite equations. The finite elements should be large enough in number to capture the approximate solution for the entire domain. The elements are connected to each other either by points (nodes), lines, or surfaces. Following this, each element in the domain is characterized by an interpolation or basis function to solve the weak form of the governing partial differential equation. A global system of equations, also known as a stiffness matrix, is formed once the equations for each element in the domain are generated and the boundary conditions are imposed. The overall system of linear equations is solved by matrix formulation utilizing the sparse matrix that minimizes the storage demand and central processing unit (CPU) time needed to compute the set of linear equations.

Finally, the system of linear equations is solved by the complex bi-conjugate gradient method to determine the values of the dependent variable at various points across the domain.55,56

One of the practical advantages of FEM is that it offers excellent flexibility for problems with geometrical and material nonlinearity. This makes it easier to optimize and predict mechanical properties like strength and toughness even before making the real prototypes, which helps in designing materials with tailored properties similar to those found in natural materials. However, FEM comes with certain drawbacks. Misinterpretations or oversimplifications of material properties, geometry, or boundary conditions during the model creation can give misleading results. In addition, the method can be computationally demanding when dealing with very complex and hierarchically structured biological systems. While FEM can provide valuable mechanical insights into the system's mechanical behavior, its reliance on accurate model assumptions may affect the accuracy of results, particularly in complex or large-scale biomimetic structures. Overall, it remains a robust mathematical tool and is more efficient in computation time for complex issues in science and engineering, providing efficient and cost-effective solutions for a wide range of applications.

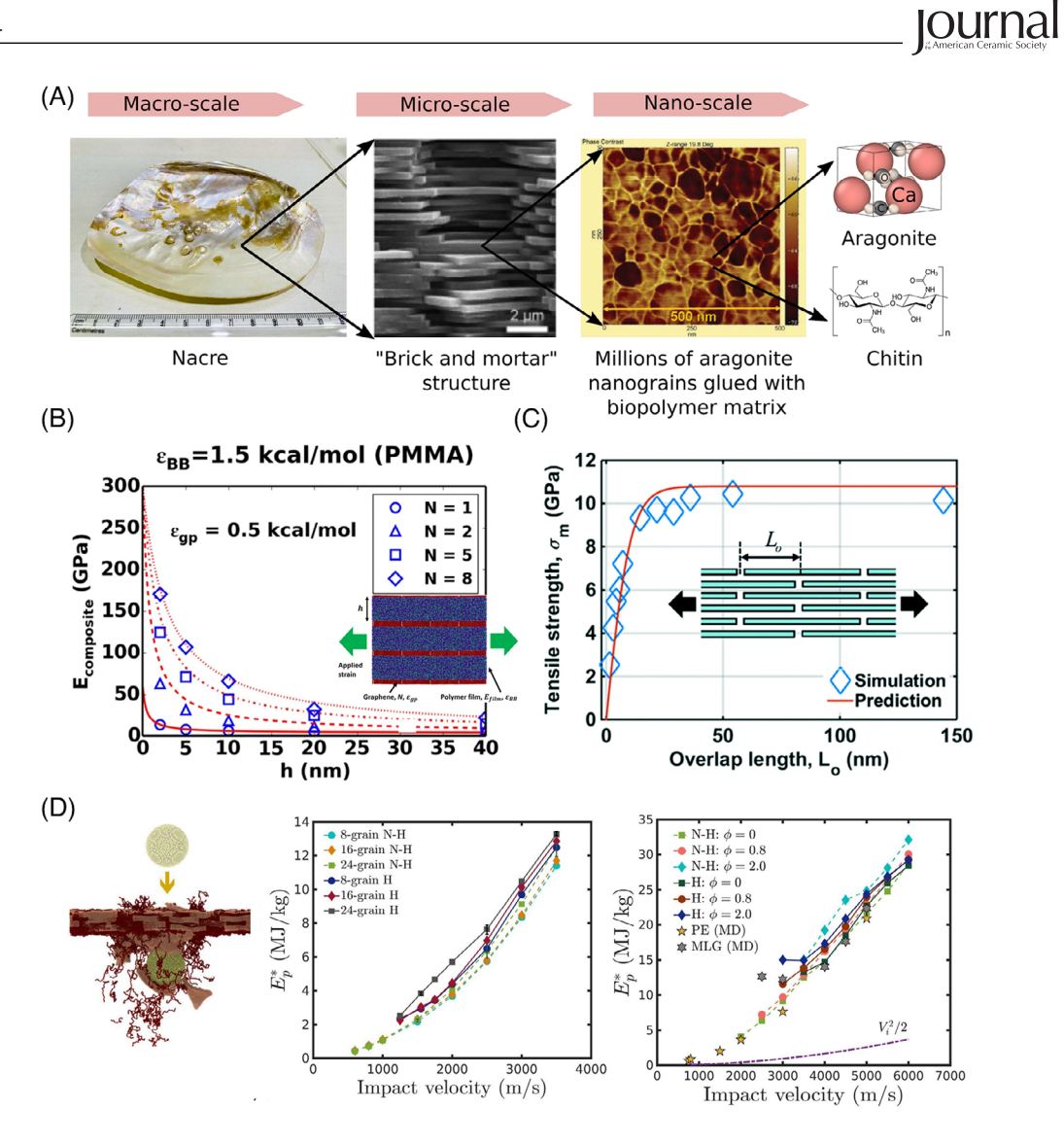
In the following sections, a comprehensive review of the recent modeling efforts for four important bioinspired structures is presented, namely, nacre, the dactyl club of the mantis shrimp, spider silk, and bone.

3 **NACRE**

Nacre, also known as mother of pearl, is a natural armor material found in mollusk shells. It is composed of ≈95 vol.% of the mineral aragonite (a crystallographic form of CaCO₃) and 5 vol.% of biopolymers.^{57–61} Over millions of years of evolution, nacre has been observed to overcome the typical strength-ductility tradeoff. The superior mechanical properties of nacre are attributed to its "brick and mortar" hierarchical structure at micro and nano length scales shown in Figure 2A. At the micro-scale, hard aragonite tablets, with widths of 10–20 μ m and thicknesses of 0.5 µm, are arranged in a staggered formation and separated by a thin layer of soft biopolymers, such as chitin and polysaccharides. Each aragonite tablet is further composed of millions of aragonite nanograins, sized 30-50 nm, bonded together by the biopolymer matrix. 62 The architecture features mineral bridges⁶³ and nanoasperities⁶⁴ at the nanoscale, with interlocked tablets⁶⁵ at the micron scale. each contributing to strengthening and toughening mechanisms. Nacre's structure can be further classified into columnar and sheet nacre based on the stacking mode of

, Wiley Online Library on [23/09/2025]. See the Term

nditions) on Wiley Online Library for rules of use; OA articles are governed by the applicable Creative Commons Licens



(A) The hierarchical architecture of nacre illustrated from macro to nano length scale. The "brick-and-mortar" microstructure and phase-contrast image of aragonite tablet is adapted from Ref.69, (B) stiffness enhancement in nacre-inspired graphene-PMMA composite due to nanoconfinement, (C) tensile strength versus graphene overlap length analyzed via CGMD simulation and compared with the shear-lag model, and (D) ballistic impact performance of nacre-inspired graphene-polyethylene nanocomposites: comparison of specific penetration energy with and without the effect of hierarchy and grafting. Reproduced with permission. 70-72

aragonite tablets in different shell-forming mollusks. The columnar structure, found in gastropods, features nucleated tablets in the same orientation as the underlying layer. As the tablets grow, they maintain this alignment, resulting in a columnar nacre with little to no overlap between the tablets. In contrast, sheet nacre in bivalves exhibits a staggered arrangement of tablets with significant overlap of tablets in adjacent layers. The variation in the organization of aragonite tablets within nacre results in distinct mechanical behavior. 66-68 Consequently, comprehending the stacking arrangement of these tablets is essential, as it provides insights for developing nacre-like composites with enhanced mechanical properties.

The micro-mechanical properties of nacre were first characterized in the 1970s, 73 and subsequent studies have

explored its mechanical behavior under various loading conditions. Under tensile elongation, nacre exhibits an initial elastic response followed by strain hardening until failure.⁶⁸ Hydration enhances toughness by increasing failure strain, while dry nacre, with Young's modulus of ≈70 GPa and tensile strength of ≈150 MPa, fails in a brittle manner due to abrupt mineral bridge fracture and tablet unlocking. Shear resistance in nacre arises from interfacial sliding between tablets, with a measured shear strength of ≈30 MPa.⁷⁴ Under quasi-static compression, nacre demonstrates elastic behavior up to ≈0.5% strain, with a compressive strength of 350-580 MPa, depending on strain rate.74 Toughening mechanisms include crack deflection, micro-buckling, tablet pullout, and organic layer deformation. At the nanoscale, the primary

toughening mechanism is energy dissipation via platelet sliding. 59,68,75 Initially, energy is dissipated through interfacial delamination and micro-crack formation, followed by mechanisms such as crack deflection, tablet interlocking, mineral bridge failure, and viscoelastic dissipation within the polymer matrix. Experimental and simulation studies using AFM, in-situ transmission electron microscopy (TEM), and MD simulations have revealed that the modular protein structure in nacre enhances energy dissipation through protein domain unfolding. 76,77 Nanoscale deformation of aragonite grains and viscoelastic behavior of the organic matrix further contribute to nacre's toughness. 78,79 Overall, platelet sliding at the submicrometer scale, regulated by nanoscale interactions, is the key mechanism underlying nacre's exceptional mechanical properties.

3.0.1 MD studies

Though numerous experimental efforts have been carried out in developing nacre-like artificial materials, understanding the fundamental atomic and molecular mechanisms underlying deformation and failure remains challenging. Consequently, atomic and molecular simulations are crucial for elucidating the structure-property relationships in these materials. In recent years, the brickand-mortar structure of nacre has consistently been the focus for synthesizing layered and staggered hierarchical composites. MD studies have been extensively employed to explore material selection, with the hard phase modeled as bulk materials like clay and ceramics, as well as 2D structures such as graphene and MXenes, while the soft phase includes polymers, glass, and similar materials. In addition to choosing the appropriate building materials, interfacial design is crucial for achieving superior mechanical properties in layered materials. Interfacial modifications, such as filler alignment, high hard-phase content, 80,81 reinforcement with bridges, 82,83 and ternary structure, 84 have been found to enhance the mechanical properties of 3D bulk nacre-like composites.

The influence of microstructure and the interaction between hard and soft phases in a brick-and-mortar nacre-like structure were analyzed using MD simulations. The findings indicate that the staggered arrangement of the hard phase enables the modulation of mechanical properties. 85,86 As shown in Figure 2B, polymer nanoconfinement induced stiffness enhancement in nacre mimetic graphene/PMMA composite was examined via CGMD simulations.⁷⁰ Overall, the trend estimated from the CGMD simulation correlates closely with experimental results on bioinspired multilaminate GO/PMMA composite. Both show that the strength and modulus increase

as the PMMA layer thickness decreases, reaching a maximum at 36 nm, with average composite strength and modulus of 278 MPa and 36.7 GPa, respectively. 87 In a study utilizing GGMD on a nacre-inspired graphene/PMMA composite consisting of 100-monomer PMMA chains and graphene sheets arranged in a staggered configuration with a 50% overlap between flakes, the interfacial failure mechanisms were examined through pull-out and the yielding of graphene layers. This evaluation highlighted how these mechanisms contribute to the composite's improved toughness and energy dissipation, as shown in Figure 2c. The molecular mechanisms identified the critical number of graphene layers at which the primary failure mode transitions from graphene yielding to pull out, leading to enhanced toughness. 71 The significance of graphene overlap in multi layered graphene is also analyzed via MD simulations. It was quantitatively predicted that, in staggered multi-layered graphene structures, a critical overlap length between graphene sheets governs mechanical performance. Characteristic overlap lengths of \approx 17, \approx 400, and ≈50 nm correspond to the strength, toughness, and failure strain, respectively.88,89 The nanoconfinement of the polymer phase within the brick-and-mortar structure was also investigated using graphene and polyethylene. The results demonstrated the enhanced yield strength (\approx 590 MPa) and toughness (\approx 120 MJ m^{-3}) for the interfacial adhesion of 0.12 Jm^{-2} of the nanocomposite with polyethylene phase confined to a 3 nm space. The CGMD simulations further show that beyond a certain polymer phase thickness of 5 nm, there is only a slight increase in toughness.90

Steered molecular dynamics (SMD) simulations were employed to investigate mineral-organic interactions between nacreous tablets, modeling the glycine-serine domain of Lustrin A. Results indicated that protein unfolding required significantly greater work near aragonite.⁹¹ MD and SMD simulations were used to examine the role of proteins in nacre fracture under uniaxial tension. The mineral-protein composite exhibited significantly higher fracture work than single-crystalline or polycrystalline aragonite. While aragonite crystals failed via dislocation motion and phase transformation, the composite failed through intragranular fracture and protein deformation. The enhanced toughness was attributed to strong electrostatic interactions between proteins and aragonite nanograins, along with the high ductility of the protein.⁹² To investigate the mechanisms involved in polymer pullout failure during deformation, a study on epoxide-rich graphene Oxide (GO) combined with a variety of polymers, namely poly(acrylic acid), poly(methyl acrylate), polyvinyl alcohol, poly(butyl acrylate), and polyethylene glycol (PAA, PMA, PVA, PBA, and PEG, respectively) provided a wealth of mechanochemical insights into the role

of the interface in determining the strength and toughness of graphene-based polymer nanocomposites. The results demonstrate that polymers with hydrogen bond donor and acceptor capabilities significantly improve toughness and resistance to failure, especially when aligned orthogonally to the loading direction. A higher concentration of hydrogen bonds increases the energy required to break the structure, resulting in stick-slip behavior in the stressstrain response.⁹³ These molecular simulations were also found to align well with the GO/PVA experimental system described by Soler-Crespo et al.⁹⁴ Both simulation and experimental fracture analyses demonstrate a comparable increase in GO fracture energy release rate and toughness, showing an enhancement in composite toughness by ≈200%.

Nacre-inspired layered structures have also been investigated utilizing MD to assess their high-impact resistance under high-strain-rate loading conditions. Among these, graphene-based materials with a layered structure are prime examples of high-impact resistant materials. 95-97 Recent studies on the dynamic response of these composites under shock loading have identified various physical and geometric factors that contribute to the enhanced shock dissipation and spall strength of multilayered nanocomposites. Critical factors such as the acoustic impedance mismatch at the interface, 98,99 polymer crystallinity,¹⁰⁰ microstructure, filler functionalization, and grafting at the interface 95,97,100,101 were found to influence energy dissipation and shock attenuation. Comprehensive CGMD simulations have been utilized to study the ballistic performance of nacre-like layered materials, revealing that the dynamic impact response of graphene-reinforced polymer nanocomposites is influenced by the distance between layers, the lateral spacing, and the graphene layer count in brick-and-mortar nacrelike structures. Perforation failure is mainly driven by chain scission and interchain disentanglement. 102 A recent study found that smaller grain sizes of graphene and overlapped grains improved the ballistic limit and penetration energy of the graphene-polyethylene structures similar to nacre, as shown in Figure 2D. The grafting of polyethylene chains on graphene further improved impact resistance by improving stress transfer.72

3.0.2 FEM studies

An early effort to understand the brick-and-mortar architecture and mechanical behavior of nacre was conducted by Katti's group, who modeled 3D hexagonal tablets with dimensions closely matching experimental values. The tablets were bonded using an adhesive element, and the effective elastic modulus of nacre was determined to be

23.6 GPa. 103 Mineral-mineral interaction in nacre, such as nanoasperities, tablet waviness, and interlocks, was further investigated through FEM. Nanoasperities were observed to contribute to hardening and shear resistance, while interlocks play a more significant role in preventing direct energy transfer to the organic layer, thereby enhancing the stiffening mechanism of the nacre layer. 65,104,105 These microstructural characteristics were found to facilitate deformation and toughening through mechanisms such as macroscopic shear-induced tablet sliding, crack deflection, crack bridging, and interlocking due to tablet waviness. In subsequent years, FEM-based structural analyses of nacre focused on mechanical behavior under quasistatic loading conditions, including three-point bending and nanoindentation. 68,106-110

Researchers have widely used FEM to study how different geometrical parameters impact the mechanical behavior of nacre-like structures. Among these, the nacre-like tablet aspect ratio plays an important role in determining the composite mechanical and viscoelastic behavior. Interestingly, an FEM parametric study was used to investigate the interfacial behavior and geometric parameters on the mechanical behavior of nacre-like structures. The analysis demonstrated that the mechanical performance of nacre-like structures is maximized at an optimal interfacial length-to-thickness ratio of approximately 2.4, with 50% overlap. In this model, to better capture the behavior of interfaces under load, simulations using PPR (PPR is a potential-based cohesive zone model) cohesive elements were employed. The simulation results matched the experimental data very closely, predicting a peak force of 51.2 N at 6.1 mm of displacement, with only small differences of 1% and 3%. Furthermore, the simulations accurately captured crack propagation through the specimen thickness prior to complete structural failure, thereby reinforcing the validity of the mode.¹¹¹ Additional investigations have highlighted how platelet overlap influences the effective modulus in brick-and-mortar designs. In one study, it was found that when the aspect ratio was higher than 25, the material mainly stretched during deformation. However, when the aspect ratio was less than 25, shear forces played a more important role in how the material deformed. Moreover, the mechanical properties of the interphase were shown to strongly affect stiffness, particularly within a platelet aspect ratio range of 20-30.112,113 A study focusing on the energy dissipation of the staggered structure has demonstrated that energy damping characteristic could also be fine-tuned through careful geometric adjustments. For instance, higher platelet aspect ratios have led to lower characteristic frequencies, while increasing platelet concentration or aspect ratio enhances storage modulus, as shown in Figure 3A. Overall, the optimal damping performance was achieved with small

FIGURE 3 (A) Contour plot of effective loss moduli with varying plate aspect ratio and overlap length (top), and with varying plate aspect ratio and frequency (bottom) for nacre-inspired staggered structure, (B) initial velocity versus residual velocity of the impactor applied to the original, Wavy, and inclined nacre-like architecture of boron carbide-aluminium composite, exhibiting superior impact-resistance demonstrated by inclined nacre-like structure, and (C) velocity-displacement curves show the nacre-like composite halts the projectile (residual velocity = 0 m/s), unlike the bulk design (final velocity = 1 m/s). Insets of Von-Mises stress reveal localized stress in the bulk, while the composite disperses stress over a wider area. Reproduced with permission. 114,116,117

platelet aspect ratios of 5–30 and sufficient platelet overlap, reinforcing the importance of microstructural tuning in mechanical performance. 114 Another study analyzed a 3D multilayered staggered nacre-like model enriched with interfacial cohesive zone as soft phase. The tablet aspect ratio and the role of interface were investigated. For varying tablet aspect ratio, it was demonstrated that the normalized stiffness approached 0.95 for very high aspect ratios, equivalent to the volume fraction of mineral tablets used in the model inline with other pervious computational and experimental studies. 115

Other studies focusing on interfacial mechanics revealed that surface roughness and mineral asperities can significantly enhance both strength and toughness by up to 2 or 3 orders of magnitude. This improvement is largely due to mechanical interlocking and frictional effects, regardless of the exact shape of the asperities. Notably, peak traction tends to rise with increasing aspect ratio, and both the aspect ratio and density of surface features were found to influence stiffness, strength, and overall toughness. 118 In particular, one design, an inverse dovetail geometry, proved especially effective at transferring stress across platelet interfaces, further boosting mechanical efficiency. 119 Complementary research on brick-and-mortar microstructures has also demonstrated how their mechanical response can depend heavily on orientation. For instance, a vertical organic matrix was

found to enhance stiffness under low loads but reduce it at higher loads. This trade-off helps lower strain in the tablets while still improving toughness. Under transverse loading, tablets exhibited the highest strain and energy density, particularly in the vertical matrix, whereas this pattern reversed when the load direction shifted. Additionally, the soft organic phase in nacre showed considerable local deformation, with microscopic strains exceeding the average bulk strain. When indentation was applied perpendicular to the tablet layers, resistance was greatly improved, thanks to the way deformation spread throughout the layered structure, which was further proved using the in situ TEM deformation tests. Experiments and simulations together offer valuable insights into the microscopic deformation mechanisms and their influence on macroscopic material behavior. 120

Although the response of nacre and nacre-like biomimetic materials to static and low-loading-rate dynamic loading has been widely studied computationally, there has been a recent increase in studies focusing on high-strain-rate impact conditions. Superior ballistic penetration resistance was observed by a nacre-like ceramic-polymer and metal-polymer composite compared to monolithic counterparts of equal areal density under identical impact conditions. This resistance was further enhanced by the optimal combination of tablet surface profile amplitude, surface roughness, cross-sectional area

of the mineral bridge, polymer thickness, hierarchy, and microstructure as referenced in Figure 3B. 116,121-123 The synergy between stiff and soft materials, achieved through 3D printing, plays a crucial role in energy dissipation. Validated LS-DYNA simulations with drop tower tests further confirm the reliability of this design approach. as shown in Figure 3C. The strong agreement between the experimental drop tower impact tests and FEM simulations, as shown in the force displacement and velocity displacement curves for both the bulk monolith and the nacre-like structure, validates that the nacre-like structure performs better under impact. 117 Expanding on structure-property findings, a gradient brick-and-mortar structure with varying cell sizes was developed and modeled. Pendulum impact tests and FE analysis were utilized to investigate the effect of gradient microstructures under impact loading conditions. Through simulations and experiments with varying cell sizes, the difference in energy absorbed between non-gradient and gradient microstructures was found to range from approximately 0.01 to 0.02 J. Overall, the gradient design helped spread out stress and strain more evenly, especially in the center of the structure during three-point bending impact, which led to a noticeable increase in the stored strain energy. As a result, the gradient structure exhibited significantly higher energy absorption compared to the uniform cell size staggered structure, with energy absorption increasing by up to four times as the cell size gradient increased. 124 The impact resistance of nacre-like structures was further analyzed by investigating the role of prestress. Drop tower tests on 3D printed samples and nonlinear FEM simulations identified a critical prestress of 12.5 MPa for optimal performance. The interplay between tablet sliding enhanced with prestress and reduced structural integrity induced by prestress led to optimal impact resistance at a critical level of prestress in nacre-shaped structures. 125 Thus, FE analysis has proven to be essential in identifying and understanding key design parameters of nacre-inspired structures and their impact on mechanical performance.

In conclusion, computational approaches like MD and FEM have played a crucial role in understanding and designing the nacre-inspired composites. MD studies including classical MD and CGMD have provided indepth insights into how interfacial interactions, filler content, and polymer confinement influence mechanical behavior and their underlying atomic and molecular phenomena. Specifically, the primary filler materials currently employed in the design of nacre-inspired composites include clay, alumina, reduced graphene oxide, h-BN, and MXenes. Studies on interfacial interactions have demonstrated that mechanisms such as chemical crosslinking, hydrogen bonding, ionic interactions, short-chain cova-

lent crosslinking, and long-chain covalent crosslinking can substantially enhance both the strength and toughness of these composites. MD studies have also shown that confining polymers between stiff fillers within layered structures, spaced just tens of nanometers apart, can significantly enhance the modulus and strength of nacre-like composites.

In the continuum length scale, FEM has offered valuable insights into optimizing geometrical parameters that influence the strength and toughness of nacre-like composites. Key factors identified include the aspect ratio of fillers and the critical overlap length between them. FEM has facilitated multiscale analysis of stress distribution, failure strength, and failure mechanisms, thereby providing a framework for achieving an optimized balance between stiffness and toughness.

These computational findings not only support experimental observations but also enable the predictive design of nacre-like composites with tailored mechanical properties. Future computational efforts should aim to integrate and scale-bridge atomistic to continuum approaches to fully capture the structural complexity including hierarchy involving multi-million atomic models under varying strain-rate loading conditions.

4 | DACTYL CLUB

The mantis shrimp (Crustacea, Stomatopoda) is a fascinating marine creature known for its excellent hunting capabilities. Residents of tropical and subtropical waters, these creatures are well-known for their unusual speed, power, and resilience, which make them impressive predators. 126 With their humongous raptorial appendages resembling a biological hammer, they use them to smash prey or defend themselves from predators. Its brutal weapon, the dactyl club, is sharp and spiny and an impact-resistant armor. With extreme accelerations, the dactyl's sharp tip or bulging heel can quickly strike both hard-shelled and soft-bodied prey (such as snails).¹²⁷ This impressive strike results from a unique power amplification mechanism in which a spring-like structure stores the elastic energy generated during muscle contraction and releases it during attack. 128 Moreover, the dactyl club is resilient because of its structural composition. It has a highly mineralized outer layer and a more flexible, organic-rich inner layer. This hierarchical structure provides strength and shock absorption, enabling the club to withstand repeated high-impact strikes without damage. 129,130 The key materials that make the dactyl club of the mantis shrimp strong are mineralized calcium phosphates present in the outer region of the club; beneath the mineralized layer, chitin, a natural polymer combined with proteins and

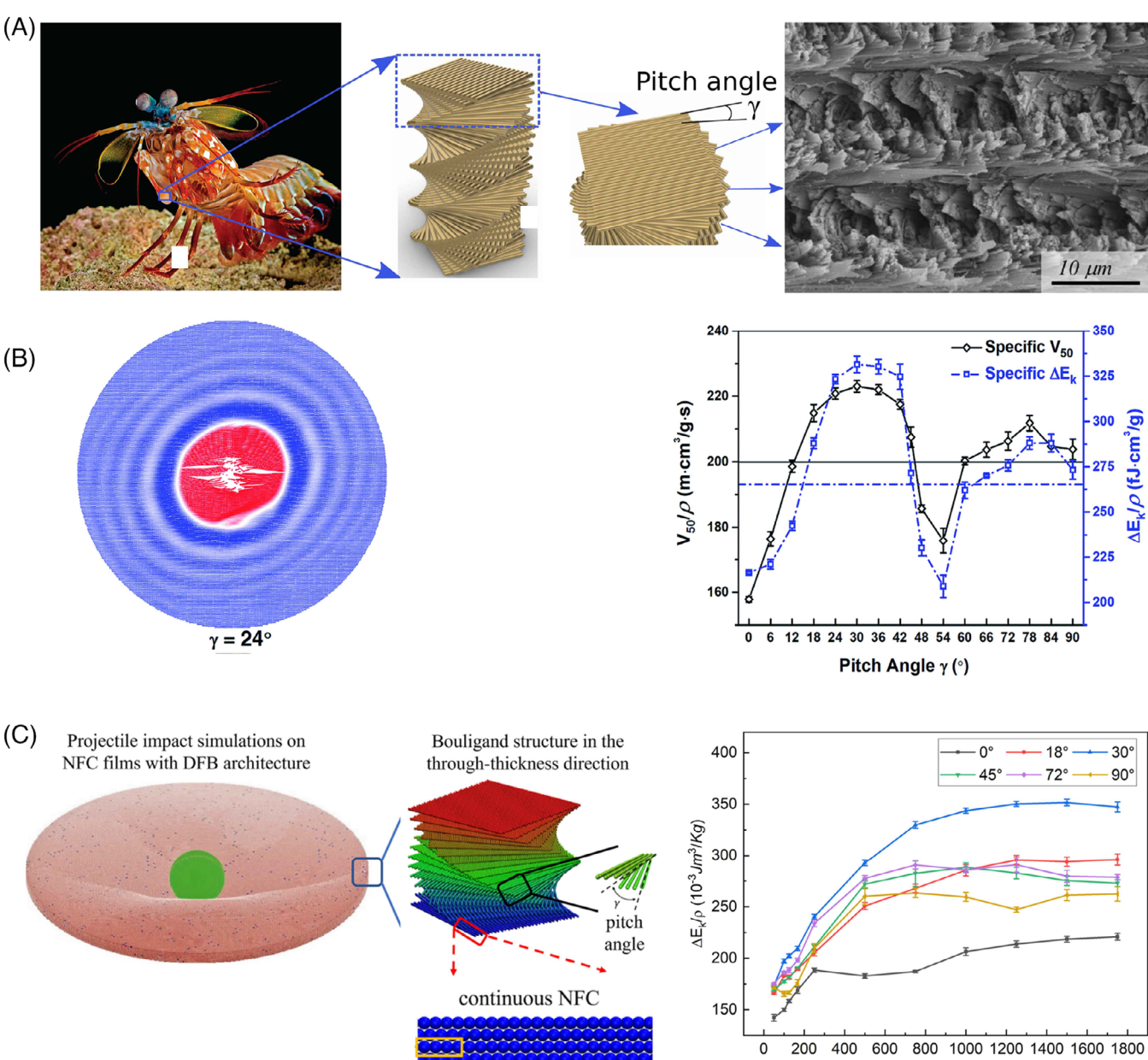


FIGURE 4 (A) Photograph of mantis shrimp with the dactyl club; 3D schematic of Bouligand structure with pitch angle and SEM image of club's fracture surface revealing helicoidal fiber organization. Reproduced with permissions. ¹³ (B) Deformation (color-coded by displacement) of nanocellulose Bouligand microstructures for pitch angle of 24°; specific ballistic limit and specific penetration energy of Bouligand microstructures with different pitch angles. Reproduced with permission from Ref. 135. (C) Snapshot depicting projectile impact on Bouligand nanofibrillar cellulose (NFC) film; the graph shows the normalized specific penetration energy of the structure for varying pitch angle versus fibre length at an impact velocity of 400 m/s. Reproduced with permission from Ref. 136.

other organic molecules, is presently responsible for a flexible framework. Moreover, the club features a highly organized, laminated structure, where layers of mineralized material alternate with organic layers. This laminated arrangement helps to dissipate energy and prevent crack propagation. The inner regions of the club have a unique helicoidal (twisted) arrangement of fibers as shown in Figure 4A, which further enhances the toughness and

damage tolerance of the structure. This helicoidal architecture is typical of many natural composites and is crucial in distributing stress and resisting impacts. 134 Mantis shrimp have inspired several studies using MD simulations. These studies aim to understand the underlying mechanisms contributing to the exceptional mechanical properties of mantis shrimp-inspired structures, including high impact resistance, toughness, energy absorption, and so on.

L (nm)

4.1 **MD** studies

Various MD simulations of the helicoidal motif of the dactyl club have been carried out in the past couple of decades. A study done by Natarajan et al. 137 shows the enhancement of the mechanical performance of helicoidal cellulose nanocrystal (CNC) films by incorporating a minority fraction of long tunicate-derived CNCs (t-CNCs) into short wood-derived CNCs (w-CNCs). This approach leads to remarkable improvements in key mechanical properties, including modulus (20.2 GPa), tensile strength (138 MPa), and toughness (1.01 MJ/m³), surpassing previously reported photonic CNC materials. Through CGMD simulations, they demonstrated toughening mechanisms such as crack bridging and deflection. Additionally, the CNC films exhibit exceptional in-plane properties; their helicoidal architecture is particularly beneficial for enhancing out-of-plane characteristics such as bending modulus, hardness, and impact resistance. Experimentally, t-CNC exhibited simultaneous increases in modulus, tensile strength, elongation to failure, and toughness consistent with the CGMD predictions. Fractographic analyses via SEM further confirmed the predicted shift in failure mode from pull-out to rod rupture. Moreover, to study the ballistic impact simulations (coarse-grained) of films with helicoidally assembled CNCs, Qin et al. 135 tested the effect of the pitch angle on the impact performance of the CNC film with respect to the specific ballistic limit velocity and energy absorption. The findings reveal that optimal impact resistance occurs at small pitch angles (18° – 42°) and can be further improved by reducing CNC interfacial adhesion, enabling better energy dissipation through crack formation and interfacial sliding as shown in Figure 4B. Building on the understanding of impact resistance in Bouligand CNC films, an important question arises: can the combination of Bouligand and staggered structures in nanofibrillar cellulose (NFC) films, forming a discontinuous fibrous Bouligand (DFB) architecture, further enhance resistance to projectile penetration? Caviness et al. 136 studied the DFB structure using coarse-grained models and ballistic impact MD simulations. The optimal design includes a critical fibril length (L) of 750 nm and a pitch angle (γ) of 30°, which maximizes energy dissipation as shown in Figure 4C. Though these mechanisms compete internally, the DFB structure enhances impact resistance through fibril sliding, crack bridging, and crack twisting. The offset configuration outperforms other designs, and beyond 750 nm, impact resistance begins to saturate. While crosslinked carbon nanotube (CNT) films have been shown to enhance quasi-static mechanical properties, their effectiveness in improving ballistic impact resistance remains uncertain. Using CGMD simulations,

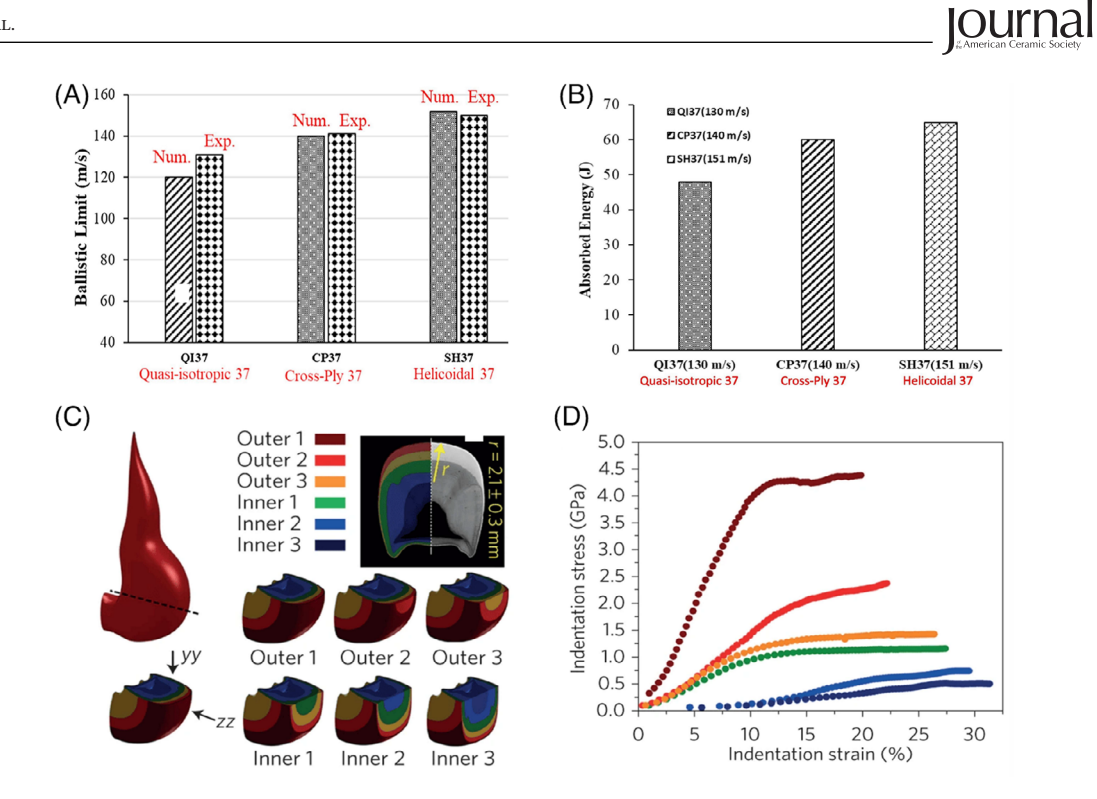
Xiao et al. 138 investigated the impact resistance of CNT film with crosslinks using micro-ballistic impact experiments. The results show that increasing crosslink density enhances energy dissipation by shifting the deformation mode from bending-dominated to stretching-bendingdominated. Crosslinks improve the interaction between adjacent CNTs, leading to a smoother penetration morphology and reduced perforation size. Higher CNT length, film thickness, and bending stiffness further enhance impact resistance, though a critical stiffness threshold exists. The study highlights crosslinking as a viable strategy to improve CNT film protective performance. Additionally, the study done by Li et al. 139 explores the impact resistance of Bouligand-like structured carbon nanotube films (BCNFs) by leveraging the helicoidal fiber arrangement. The researchers analyzed the effect of pitch angle and intertube crosslinking on energy dissipation and impact resistance, and showed that at 1 km/s impact velocity, projectiles exhibit embedding, bouncing, or penetration, while at 2 km/s, all films are penetrated. Increasing crosslinking density shifts the energy dissipation mode from interface sliding and bending to CNT fracture and collapse. The study highlights the potential of crosslinked BCNF structures in enhancing impact protection and offers theoretical insights for CNT-based protective materials. To bridge the gap between the analysis of single crack propagation in Bouligand structures and the phenomenon of damage delocalization and its subsequent toughening effect, Garnica et al. 140 investigate the influence of crack twisting on damage delocalization by conducting simulations on a Bouligand structure material under uniaxial loading conditions. The results confirm that lower pitch angles enhance damage delocalization, promoting multiple crack nucleation and reducing localization, while higher pitch angles increase strength but lead to concentrated damage. Even with 10% defects, the structures remain resilient by effectively distributing damage. The study also validates previous findings on twisting cracks, showing that they tend to remain isolated and experience restricted lateral growth. Furthermore, the coarse-grained model provides an effective and practical method for analyzing and understanding the fracture mechanics of complex fiber-reinforced composites. Wu et al. 141 performed a computational as well as experimental analysis of Bouligand biomimetic ceramic composites reinforced with carbon fibers. FEM simulations were used to study crack propagation and stress distribution under threepoint bending, revealing that fiber orientation significantly influences fracture behavior. Peridynamic simulations further confirmed that a 0° fiber arrangement effectively blocks crack extension, while a 90° arrangement promotes it. MD simulations analyzed interfacial bonding,

showing stronger polymer-Al₂O₃ adhesion compared to polymer-CF, validating experimental observations of fiber debonding. The results indicate that optimized fiber orientations enhance energy dissipation, improving fracture toughness by 62.4% and bending strength by 12.2%, contributing to the development of high-strength, damageresistant composites. Moreover, a strong correlation is observed between experimental findings from microstructural analysis (via SEM and X-ray diffraction) and simulation outcomes obtained through FEM and MD. The experimental observations confirmed the presence of grain refinement, improved phase distribution, and mechanical strengthening mechanisms such as dislocation pinning and grain boundary sliding. These phenomena were mirrored in the FEM results, which simulated localized stress distribution and deformation under load, and in the MD simulations, which captured atomic-scale interactions and dislocation dynamics. Together, these results validate the predictive accuracy of the multiscale simulation approach and reinforce the experimentally observed improvements in strength and ductility of the processed material.

4.2 **FEM studies**

The study by Suksangpanya et al. studied crack growth in helicoidal composites, combining experiments, theory, and simulations. 142 They found that twisted cracks shaped by fiber layout—boost fracture resistance by delaying crack initiation and preventing further propagation. This happens due to shifted fracture modes and larger crack surfaces. FEM revealed stress patterns, showing cracks grow faster near their rotation center, building on earlier work about helicoidal laminates' strength. One such study was conducted by Liu et al. 143 The study investigates the damage behavior of helicoidal and cross-ply laminates under transverse loading using experiments and computational simulations. Cross-ply laminates develop multiple small delaminations due to lower interlaminar shear strength, leading to several load drops as cracks propagate. In contrast, helicoidal laminates form a single large delamination at the mid-plane, delaying failure and achieving a 30% higher peak load. FEM helped track damage evolution, showing that introducing additional delamination above the mid-plane forces cracks to travel further, further increasing peak load. The study by Taydon et al.¹⁴⁴ investigated the bilayer saddle structure of mantis shrimp. Through micro-mechanical testing and FEM analysis, they found the saddle distributes stress efficiently, keeping the outer layer elastic and preventing failure. The simulations aligned with experimental crack patterns, confirming the design's effectiveness. However, limitations such as simplified geometry and omission of viscoelastic effects affected the accuracy of energy release predictions. With a focus on applications in the design of armor, aerospace, and automotive structures, Abir et al. 145 studied the impact resistance and energy absorption of bioinspired helicoidal composites modeled after the mantis shrimp's endocuticle. Using numerical modeling, researchers analyzed how the helicoidal architecture enhances ballistic performance compared to conventional laminates. The results showed that a 37-ply helicoidal composite had an 8% and 15% higher ballistic limit (151 m/s) than crossply (140 m/s) and quasi-isotropic (130 m/s) laminates, respectively, as shown in Figures 5A and B.

The study by Jiang et al.¹⁴⁷ investigates carbon/epoxy composite laminates to improve impact resistance. They tested four helicoidal layups with varying rotation angles using finite element simulations in ABAQUS. The results showed that increasing the rotation angle between plies delayed damage onset and improved energy absorption. Helicoidal-Recursive (HR) and Helicoidal - Exponential (HE) layups with larger rotation angles performed best, with less damage and better stress distribution. Crack paths also shifted with fiber orientation, boosting damage tolerance. Liu et al.¹⁴⁸ examined the impact resistance of helicoidal laminates with constant and nonconstant inter-ply angles inspired by the mantis shrimp's exoskeleton. Carbon fiber-reinforced polymers (CFRPs) with graded helicoidal structures were tested under outof-plane loading. FEM showed that small inter-ply angles resist delamination, while larger angles prevent matrix splitting under tensile bending. Laminates with a nonconstant inter-ply angle outperformed cross-ply laminates by up to 75%. The study from Mencattelli and Pinho¹⁴⁹ explored the impact resistance of thin-ply CFRP laminates. Low-velocity impact and compression after irmpact tests were conducted on laminates with pitch angles ranging from 2.5° to 45°, revealing that smaller pitch angles improve damage tolerance by diffusing sub-critical damage, reducing delamination, and delaying fiber failure. The best-performing configuration had a 13.3% higher peak load and a 34.9% larger displacement at load drop than standard configurations. Moreover, to study the ballistic performance of the helicoidal laminates, Liu et al. 150 examined the ballistic performance of helicoidal laminates, inspired by the mantis shrimp's exoskeleton, using carbon-epoxy Kevlar-epoxy and polyethylene fiber laminates. Experimental and numerical simulations revealed that helicoidal carbon-epoxy laminates with small interply angles outperform cross-ply and quasi-isotropic laminates, absorbing 32.6% and 86.6% more impact energy, respectively. However, due to different failure mechanisms, helicoidal Kevlar-epoxy and polyethylene laminates performed worse than their cross-ply counterparts.



(A) Comparison between experimental and numerical ballistic limit and (B) absorbed energy at penetration for quasi-isotropic, cross-ply, and helicoidal configurations. Reproduced with permission from Ref. 145. (C) Schematic cross-section of the club at various indentation locations, and (D) indentation stress-strain curves in dry conditions from the partial loading-unloading. Reproduced with permission from Ref. 146.

FEM showed that helicoidal laminates mainly fail through matrix splitting, with projectiles crushing front-face fibers and slipping through rear cracks. Cross-ply and quasiisotropic laminates, however, fail mostly by fiber breakage. This suggests helicoidal designs suit brittle fibers best, while tougher fibers perform better in cross-ply setups. Building on this understanding, Han et al. 151 introduced a novel helical-fiber sinusoidal-structure laminate (HSL) using unidirectional basalt fiber prepreg. Through lowvelocity impact experiments and finite element simulations, they found that HSL offered significantly better impact resistance compared to other configurationsincluding unidirectional-fiber flat (UFL), unidirectionalfiber sinusoidal laminate (USL), and helical-fiber flat (HFL) laminates. The HSL achieved the highest peak impact force of 6593.45 N, representing increases of 65.29%, 108.05%, and 13.00% over UFL (3988.80 N), USL (3169.21 N), and HFL (5835.20 N), respectively. Remarkably, it also showed the least damage among all configurations. These results were supported by finite elemental analysis (FEA), which demonstrated that the helical fiber layout helped resist crack propagation, while the sinusoidal structure improved energy absorption under impact.

Further advancing this field, Yang et al. 152 examined biomimetic Bouligand-type helicoidal CFRP laminates using multiscale FE modeling to predict low-velocity

impact resistance and energy absorption. Their models incorporated both material uncertainties and pitch angle variations, offering realistic simulations that matched well with experimental outcomes. Sensitivity analyses revealed that fiber longitudinal elastic modulus and fiber volume fraction had the greatest effect on peak impact loads, while energy dissipation was mainly governed by the fiber modulus. Notably, smaller pitch angles and higher fiber moduli led to improved impact resistance and energy absorption capacity. Chau et al.¹⁵³ explored the fracture mechanics of the mantis shrimp's highly mineralized dactyl club, a natural impact-resistant structure. They employed microcantilever bending tests with chevronnotched cracks to analyze crack propagation more reliably than traditional nanoindentation methods. Using both linear elastic (LEFM) and elastic-plastic (EPFM) fracture mechanics, they found a marked difference in toughness values: 0.21±0.08 MPa.m^{0.5} (LEFM) and 1.89±0.41 MPa.m^{0.5} (EPFM). This indicated that plastic dissipation at the crack tip was the dominant toughening mechanism in the dactyl club's impact zone. A similar study was carried out by Amini et al., 146 as shown in Figures 5C and D. In their study, Yang et al. 154 explored the intricate hierarchical structure of the mantis shrimp's tail spike, focusing on its chemical composition, microstructure, and mechanical behavior. They found that the outer and inner exocuticle layers feature helically arranged and

circumferentially aligned fibers, which play a key role in guiding cracks along the spike's length. This extended crack path helps maximize energy dissipation by increasing the strain energy released during fracture. To test the impact of this structural design, the researchers created 3D-printed biomimetic models. These tests confirmed that combining Bouligand-type architectures with radially aligned parallel fiber layers significantly improves both strength and toughness. The results highlight how nature's multiscale design strategies can inspire high-performance synthetic materials that are both strong and damagetolerant.

The study by Yang et al.¹⁵⁵ investigated the mechanical properties of mantis shrimp abdominal segments by fabricating a helicoidal structure using laser powder bed fusion, achieving high precision (7 μ m peak deviation) and density (99.78%). The structure exhibited 2.4 times greater specific energy absorption (14.3 J/g) and 2.7 times higher plateau stress (68.4 MPa) than standard honeycomb and tube designs. The best performance was observed at a 45° rotation angle with three layers, attributed to the twisted stress conduction path that enhanced load distribution. Moreover, the results strongly correlate with the experimental data. Experimental techniques like SEM revealed a multiregional composite structure with helicoidal and impact-resistant zones, showing distinct crack deflection and energy dissipation patterns. These findings were reinforced by FEM simulations, which demonstrated how stress waves propagate differently through each structural region. The study by Eltaher et al. 156 focused on helicoidal composite plates, examining their static stability and vibration behavior. Using FEM with ANSYS, researchers explored how factors like fiber orientation, slenderness ratio, elasticity ratio, and boundary conditions influenced performance. They found that lamination layup had a strong effect on static deflections and stress distribution, and that natural frequencies tended to decrease as plate thickness increased. Among the configurations, quasiisotropic and linear helicoidal designs showed higher vibration frequencies, whereas unidirectional and crossply layouts exhibited lower frequencies. Changing the spiral angle results in the distribution of stress components, which was studied by Zhang et al.,157 wherein they examined how adjusting the spiral angle affects stress distribution in beam-shaped composites inspired by the mantis shrimp's claw rod. They designed six beam models with varying interlayer rotation angles to study these effects. Their findings showed that smaller spiral angles improved strength but reduced energy absorption, highlighting a trade-off between toughness and durability. Simulations revealed that changing the spiral angle alters internal stress patterns—lower normal stress boosts strength, while higher shear stress supports toughness.

The best performance was achieved with interlayer angles between 4° and 5°, where both high strength and toughness were maintained.

Pro et al.¹⁵⁸ explored how Bouligand and cross-ply fibrous laminates respond to fracture, using the discrete element method (DEM). The results showed that while Bouligand structures tend to twist cracks, this mechanism was less effective at improving toughness compared to crack pinning in 0°/90° cross-ply laminates, which helped spread damage across a larger volume. DEM simulations further revealed that all architectures performed similarly when using weak fibers, but for stronger fibers, cross-ply designs offered better resistance to fracture. The Bouligand layout showed a slight increase in toughness at pitch angles between 20žand 30°, though it consistently fell short of the toughness provided by cross-ply laminates across different crack directions. Dong et al. 159 explored the impact resistance of the mantis shrimp using a combination of in situ high-speed X-ray imaging, nano-CT, and dynamic finite element modeling, uncovering a previously unknown 3D interlocking structure in the impact region, where mineral-coated surfaces and fiber bundles form a suture-like transition zone that helps prevent cracks from spreading uncontrollably. The study also emphasized the importance of in-plane and out-of-plane pore canals, which are reinforced with mineral particles and contribute to energy dissipation by encouraging multiple crack initiation points. Dynamic simulations supported these findings, showing that the interlocking architecture and stiffness mismatches between regions work together to deflect and slow crack growth. They also found that hydration plays a major role; hydrated samples exhibited more plastic deformation, greater fiber bridging across scales, and increased particle breakage compared to dry ones.

Yang et al. 160 examined the fracture of Bouligand-type structures, focusing on two configurations: the singletwisted (SBS) and double-twisted (DBS) designs found in natural materials like ancient fish scales. Using extended finite element modeling (XFEM) in ABAQUS, they simulated single-edge notched tensile tests to study how these structures respond to stress and displacement. They showed that the DBS configuration offers much better fracture resistance and toughness than SBS, largely due to its ability to limit damage within layers and more evenly distribute stress between them, particularly at smaller pitch angles. The presence of interbundle fibrils in DBS also played a key role in boosting interlaminar strength, leading to better overall fracture performance. Nie and Li¹⁶¹ developed a multiscale fracture model to better understand how Bouligand structures resist cracking, taking into account material inhomogeneity, anisotropy, and multiscale characteristics. FE simulations validated their findings, which highlighted two main toughening mechanisms: first, the

15512916, Q. Downloaded from https://ceramics.onlinelibrary.wiley.com/doi/10.1111/jace.70241 by Raghavan Ranganathan - Indian Institute of Technology Gandhinagar, Wiley Online Library on [23.99.2025]. See the Terms and Conditions (https://onlinelibrary.wiley.com/erms

and-conditions) on Wiley Online Library for rules of use; OA articles are governed by the applicable Creative Commons License

multiscale structure and uneven material properties help relieve stress around the crack tip; second, the twisting of cracks shifts the loading from a single mode to a mixed-mode state, improving toughness.

In summary, MD simulations, particularly in their CGMD form, have been employed to study the toughening and impact resistance mechanisms of the dactyl club's helicoidal architecture. These simulations have not only replicated but also explained experimental findings, demonstrating how structural parameters such as pitch angle, fibril length, and interfacial adhesion govern energy dissipation through mechanisms like crack bridging, deflection, twisting, fibril sliding, and interfacial sliding. By simulating atomic to mesoscale phenomena, MD provided insights into interfacial bonding strengths, fracture behavior, and damage delocalization that would be challenging to isolate experimentally. Importantly, these computational results consistently correlated with experimental outcomes, validating MD as a predictive tool while also offering a platform to explore design variations such as discontinuous fibrous Bouligand arrangements, which are beyond current fabrication capabilities. This synergy between MD simulations and experiments strengthens the design framework for bioinspired, high-performance impact-resistant composites.

FEM has been widely applied to study the dactyl club, enabling researchers to link structural motifs to mechanical performance under various loading conditions. These simulations have been instrumental in revealing how helicoidal fiber architectures, sinusoidal interfaces, and hierarchical arrangements influence stress distribution, crack initiation, and energy dissipation. Furthermore, advanced studies have applied FEM to parametric variations in rotation angle, fiber orientation, and laminate lay-up, showing that small pitch angles can enhance delamination resistance while larger ones reduce matrix splitting. Beyond laminate mechanics, FEM has been integrated with fracture mechanics approaches to simulate crack propagation in Bouligandtype architectures, validating experimental crack paths and toughening mechanisms such as mixed-mode loading.

While FEM provides valuable predictive insights, the reviewed studies also highlight limitations. Many models use simplified geometries, idealized boundary conditions, or omit rate-dependent and viscoelastic effects, which can limit accuracy in replicating biological conditions.

5 SPIDER SILK

Spider silk—often called nature's super fiberhas long fascinated researchers because of its remarkable mechanical performance. Spiders spin this versatile material for tasks like building webs, catching prey, and safeguarding their eggs. What sets spider silk apart is its rare balance of strength, stretchability, and toughness, outperforming most man-made and natural fibers. 162

Major ampullate (MA) silk, often called dragline silk, stands out for its impressive strength—comparable to steel—and elasticity similar to rubber. 163 This rare combination makes it incredibly tough, allowing it to absorb much more energy before breaking than common synthetic fibers like Kevlar or Nylon.¹⁶⁴ The remarkable mechanical properties of spider silk come from its hierarchical structure. On a molecular level, spider silk proteins-known as spidroins-contain highly repetitive amino acid sequences that organize into crystalline β sheet regions and amorphous domains, as shown in Figure 6A.¹⁶⁵ This layout gives the silk its unique combination of strength and flexibility. 166,167 The β -sheet crystals are responsible for its high tensile strength, while the amorphous regions allow it to stretch without breaking. 168 Moreover, the amphiphilic nature of spidroins helps them align and assemble into fibers during the spinning process. 169 Spider silk's mechanical performance stands out even when compared to well-known engineering materials. Though steel can reach tensile strengths of up to 4 GPa, its high density and limited elasticity make it less efficient than spider silk on a per-weight basis. Carbon fibers, while strong, tend to be brittleunlike spider silk, which blends strength with stretchability, allowing it to withstand large deformations without breaking. 162 It also displays unusual behaviors, like shrinking when exposed to humidity (supercontraction) and having shape memory, which help it perform reliably in natural environments.^{170,171} The link between spider silk's structure and function has led to intense interest in replicating its properties. While reproducing its intricate assembly remains a challenge, progress in biotechnology and artificial spinning continues to move the field forward. 172,173 This section highlights the structural features that give spider silk its exceptional qualities and reviews current efforts to engineer silk-like materials for advanced applications.

5.1 | MD studies

The study by Venkatesan et al. 177 explored the shape memory behavior of a genetically engineered spider silk protein, eMaSp2, inspired by the supercontraction seen in natural spider silk. Using a biomimetic wet-spinning technique, they created fibers rich in β -sheet structures that closely mimic those found in nature. When tested at 75% relative humidity, the fibers showed impressive

SWCNT (wt%)

SWCNT (wt%)

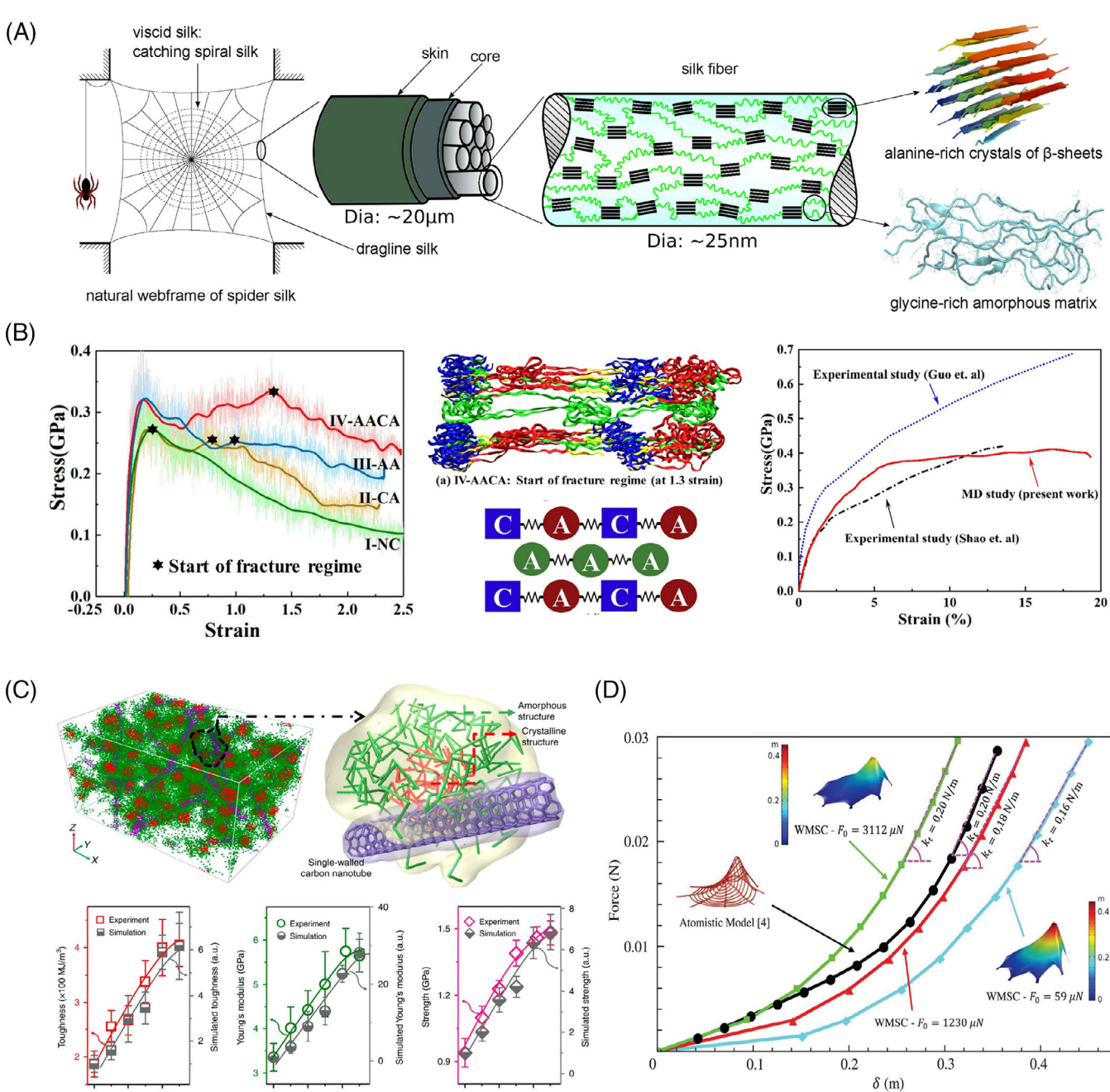


FIGURE 6 (A) Illustration of spider dragline silk architecture, showing the dragline silk composed of alanine-rich β -sheet nanocrystals within glycine-rich disordered peptide chains. Reproduced with permission from Ref. 165. (B) Stress-strain plot of the four models at 5×10⁻⁶ per fs strain rate for varying structures based on interconnectivity; Snapshots of the models at the start of the fracture regime for model AACA at 1.3 strain; Comparison of the stress-strain plot for *B. mori* silk fibroin single filament performed experimentally with the molecular model (AACA). Reproduced with permission from Ref. 174. (C) Snapshot of the coarse-grained S-silk composite: red indicates crystalline β -sheet structures, green represents amorphous regions, and purple denotes SWCNTs; Graphs illustrating that toughness, Young's modulus, and strength increase with higher SWCNT wt%, highlighting SWCNT's key role in enhancing the mechanical properties of the silk composite. Reproduced with permission from Ref. 175. (D) Force–displacement comparison of spider web atomistic model and FEM-simulated weak-matrix silk composite under transverse load on a radial thread. Reproduced with permission from Ref. 176.

SWCNT (wt%)

shape fixity (82.1%) and nearly complete recovery (98.5%). At 90% RH, the fibers achieved a high recovery stress of 18.5 MPa—surpassing many traditional shape memory polymers and composites. MD simulations over 200 ns supported these findings by revealing that hydrogen bonds in the amorphous regions acted like switches, triggering the contraction. In addition, the experimental studies demonstrate the macroscopic properties, such as shape memory behavior, mechanical strength, and structural features, revealing how the fibers respond to humidity and mechanical stress. These results offer promising insights for designing smart materials that respond to humidity, with potential applications in responsive and functional materials. Additionally, the study by Asakura¹⁷⁸ provides a comprehensive overview of recent progress in understanding the structure and behavior of spider dragline silk, drawing on insights from solid-state nuclear magnetic resonance (NMR) and MD simulations. Since spider silk lacks a fully crystalline structure, conventional diffraction techniques fall short in capturing its molecular details, making NMR and MD essential for probing both the ordered and disordered regions at the atomic scale.

MD simulations, in particular, have proven valuable for linking the interplay between crystalline and amorphous domains to the silk's mechanical performance. Together, these techniques have deepened our understanding of silk's behavior in both dry and hydrated environments and are contributing to the development of next-generation biomaterials. Building on this, Kim et al. 179 used MD to examine how hydration levels influence the mechanical properties of spider silk. By analyzing the crystalline and amorphous regions of MaSp1 and MaSp2 proteins, researchers found that wild-type (WT) silk outperforms modified models, particularly at 50% hydration, due to its stable β -sheet structures. The CGMD simulations revealed that WT silk maintains strength and toughness by optimizing water collection and hydrogen bonding. The findings highlight the silk's resilience to hydration fluctuations, which is crucial for capturing prey. This research provides insights into natural materials and their potential applications in bioinspired designs. Moreover, the study by Rawal et al. 180 focuses on the mechanical properties of nanoscale spider silk protein (3LR2) using SMD simulations. Researchers analyzed fraying deformation and tensile strength by pulling on the β -chain in the x-direction while keeping the other end fixed. The Gibbs free energy for complete chain separation was calculated as 18.59 kCal/mol, indicating strong intermolecular interactions. Tensile stretching simulations revealed an elastic modulus of 20.136 GPa at a strain rate of 11.65. MD simulations, including center-of-mass pulling and umbrella sampling, further confirmed the protein's high mechanical strength and stability. These findings provide valuable insights for

developing bioprinted composite spider silk biomaterials with enhanced properties for biomedical applications.

Furthermore, Chang et al. 181 developed a high-strength, ultra-tough sov protein (SP)-based material inspired by the nanoconfinement effect in spider silk. By using tannic acid (TA) as a hydrogen bond cross-linker between hyperbranched polyester (HBPE) and the SP matrix, a dynamic nanoconfinement phase was created, mimicking the β -sheet reinforcement in natural silk. The resulting SP/HBPE/TA film achieved a tensile strength of 44.6 MPa and an ultrahigh toughness of 44.7 MJ/m³, surpassing other bio-based materials and outperforming plastic-based materials. Molecular interactions, analyzed through Hbond dynamics, contributed to its excellent recyclability, water resistance, UV shielding, and antibacterial properties. This biomimetic approach provides a promising alternative to plastics, supporting sustainable material development and waste reduction efforts. The CGMD study done by Bashusqeh et al. 182 developed the MD model to investigate the mechanical properties of spider silk, specifically focusing on MA silk proteins (MaSp1). The study utilized a systematic approach, where MaSp1 chains were subjected to uniaxial tensile loading, and the results from the CG model were compared with all-atom simulations to validate its accuracy. The findings revealed that the average density of the simulation box was 1.28 g/cm³ for the CG model and 1.25 g/cm³ for the all-atom model, indicating a strong agreement with experimental observations. Additionally, the longitudinal length of the simulation box during equilibration was measured as 114.6 Å for the CG model compared to 110.2 Å for the all-atom simulations. The results demonstrated that simulating multiple bundles of MaSp1 chains led to increased density and longitudinal length, reflecting more realistic structural properties of spider silk. This research establishes a mechanically consistent CG model and provides a framework for future studies in silk protein engineering and bioinspired material design.

Shin et al.¹⁸³ investigated the effects of electric fields on the mechanical properties of spider silk from Nephila clavipes. The methodology employed MD simulations to analyze how varying electric field amplitudes and orientations impact the β -sheet structure of the silk, which is crucial for its mechanical integrity. The results indicated that while higher electric fields generally led to decreased mechanical properties, an electric field of 0.1 V/nm applied in the antiparallel direction improved both Young's modulus and ultimate tensile strength (UTS). Specifically, this condition preserved structural integrity and minimized disruptions to hydrogen bonds, vital for maintaining silk's strength. The study concluded that optimizing electrospinning conditions, such as lowering power levels, could enhance silk fiber production and applications by

preventing structural disruptions compromising mechanical properties. These findings highlight the delicate balance between electric field application and the preservation of silk's unique mechanical characteristics, suggesting that careful control during electrospinning can lead to superior performance in biomaterial applications. Moreover, Zhao et al. 184 investigated the interfacial interactions between cellulose and spider silk protein (NTD) using MD simulations to optimize cellulose/spider silk protein composites for biomedical applications. Simulations performed using the GROMACS-5.1 software with the CHARMM36 force field revealed that NTD proteins adsorb spontaneously onto cellulose surfaces while maintaining their structural integrity. Van der Waals and hydrogen bonding interactions were identified as key drivers of protein binding, though the adsorption was not highly stable. The findings suggest that modifying cellulose surface properties, such as increasing hydrophilicity, could enhance protein binding and composite performance. These insights provide a theoretical foundation for designing biocompatible and degradable cellulose/protein composites for tissue engineering, drug delivery, and medical dressings. Furthermore, Yuan et al. 185 studied the mechanical properties of spider silk proteins MaSp1 and MaSp2 using AlphaFold3 models and all-atom MD simulations. SMD simulations revealed that MaSp1 exhibits superior extensibility, forming cavities under longitudinal stress, while MaSp2 provides greater toughness with uniform stretching and higher lateral tensile resistance. Hydrogen bonding analysis showed that GLN and SER bonds in MaSp1 contribute to its extensibility, whereas weaker Tyr307 bonds reduce toughness. In contrast, MaSp2 maintains uniform stretching through Gly-Ser interactions, enhancing its rigidity. These findings provide molecularlevel insights into spider silk's strength and toughness, guiding the design of artificial fibers and biomaterials. Moreover, Patel et al. 174 studied the Bombyx silk fiber (B. mori SF), a biopolymer, wherein they simulated four different phenomenological models to study tensile strength, elastic modulus, and stress-strain as shown in Figure 6B. A study by Pan et al.¹⁷⁵ employed dissipative particle dynamics-based CGMD simulations to understand supertough electro-tendon based on spider silk supertoughened by single-walled carbon nanotubes (SWCNTs). As shown in Figure 6C, toughness, Young's modulus, and strength increase with increasing weight fraction of SWCNTs.

FEM studies 5.2

Jiang et al. 186 use a multiscale modeling approach to analyze the dynamic response of spider orb webs during prey capture, incorporating both microstructural mate-

rial properties and macro-scale aerodynamic effects. FE simulations reveal that energy dissipation occurs through material damping mechanisms, including viscoelasticity, α -helix chain fracture, and β -sheet unfolding, which dominate for small prey. Aerodynamic drag becomes the primary energy absorption mechanism for prev. reducing oscillations and potential web damage. The findings highlight the critical role of silk microstructure in impact resistance and provide insights for designing biomimetic capture systems. Furthermore, Xu et al. 187 studied a bioinspired flexible web system for space debris capture, modeled after the structure and performance of spider webs. Using image processing, a cobweb-like flexible structure was designed and analyzed using FEM to compare its capture efficiency with traditional quadrilateral webs. Ground experiments validated the bionic design's superior mechanical properties, energy dissipation, and fault tolerance. The results confirm that the octagonal flexible web significantly enhances capture performance compared to traditional quadrilateral webs, providing theoretical and experimental foundations for future space debris removal systems.

The study by Fraternali et al.¹⁸⁸ develops a tensegrity model to explain the mechanical behavior of spider dragline silk, focusing on its hierarchical organization into microfibrils with radially varying properties. Using air plasma etching and low-voltage SEM imaging, the model successfully captures key experimental observations, including the Poisson effect, tensile stress-strain response, and enhanced fracture toughness. The model describes fibrils as chains of polypeptide tensegrity units, where crystalline granules (under compression) are linked by amorphous segments (under tension), demonstrating that radial variations in ductility enhance toughness through crack-deflection and crack-stopper mechanisms. Future work will refine the model by incorporating rate- and humidity-dependent properties, fibril twisting, shear, and bending modes, and super contraction effects, ultimately guiding the design of biomimetic fibers with optimized toughness and structural grading. The study by Jiang et al. 189 develops a constitutive model for spider dragline silk, incorporating its hierarchical microstructure of soft α -phase and reinforcing β -fillers. Using only seven material constants, the model accurately captures strain stiffening, viscoelasticity, Mullins effect, and plastic deformation. FE simulations validate the model, reproducing the S-shaped stress-strain response observed experimentally. Key findings show that increasing chain density stiffens the material, while a higher Kuhn number enhances flexibility. The results provide insights into silk's energy dissipation and mechanical behavior, aiding biomimetic material design. Kaewunren et al. 190 carried out two similar kinds of studies, wherein

they first studied the free vibration behavior of spider web structures using FEM in Abagus, focusing on natural frequencies, mode shapes, and geometric nonlinearity. Large-deformation 3D FE models were developed and validated, incorporating energy-based variational models to analyze axial strain, kinetic energy, and self-weight effects. Key findings reveal that radial threads significantly enhance stiffness, while capture threads mainly add mass. Additionally, pretension loads induce nonlinear hardening effects, influencing structural stability and stiffness. The study provides insights for bioinspired structural designs, aiding in preventing dynamic resonance and failure in engineered membranes and flexible structures. Second, they¹⁹¹ examine imperfect spider web structures' nonlinear free vibration behavior using FEM in ABAQUS. The research focuses on four types of imperfections: spiral, radial, central, and circular rings, analyzing both linear and geometric nonlinear responses. Key findings reveal that pretension in spider silk significantly influences vibration characteristics, with radial thread damage having the most impact on structural behavior. Geometric nonlinearity leads to frequency shifts and structural hardening, especially in spiral and circular ring imperfections. These insights provide valuable guidance for structural engineers in designing bioinspired, high-tensile structures.

Li et al. 192 developed bioinspired spider silks using the 4D printing of shape memory polyurethane, enabling dynamically tunable mechanical properties. Two energyabsorbing mechanisms were incorporated: predefined nodes via 4D printing and stimuli-induced spiral deformation triggered by temperature, humidity, or infrared light. FEM was used to analyze the effects of these stimuli on mechanical performance, demonstrating that the shape and size of energy-absorbing units can be controlled, directly influencing tensile properties and impact resistance. The ability to dynamically adjust mechanical properties provides potential applications for bio-inspired spider webs in engineering fields requiring adaptive materials, such as aerospace, robotics, and protective structures. Adding to that study of the energy-absorbing properties, Xie et al. 193 investigate the energy-absorbing properties of bionic spider web structures using a combination of theoretical analysis and FE simulations. A bionic orb web model was developed, considering structural factors such as radial line length, cross-sectional diameters, number of spiral lines, and spiral spacing. With the help of FEM and the Box-Behnken Design method, results showed that radial line length and spiral cross-sectional diameter significantly influence energy absorption, with shorter radial lines increasing total absorbed energy. A regression equation was derived to determine the optimal structural parameters for maximum energy absorption. These findings provide valuable insights into designing

energy-absorbing structures for aerospace, automotive, and wearable applications.

Mohol et al.¹⁹⁴ developed a computational approach to analyze the mechanical behavior, fluid dynamics, and degradation of polylactic acid scaffolds with natureinspired architectures for bone tissue engineering. Five different scaffold designs (Spider-web, Sunflower, Honeycomb, Nautilus Shell, and Giant Water Lily) were evaluated using FEM and computational fluid dynamics (CFD). Results showed that the Spider-web scaffold exhibited the least deformation (0.725 μ m) and lowest stress (0.308 MPa), while the Nautilus Shell scaffold had the highest stress (3.548 MPa). Permeability values met cancellous bone requirements, and CFD analysis confirmed that wall shear stress supported cell differentiation. Degradation analysis revealed that the Spider-web scaffold degraded the slowest (9.5 weeks), while the Giant Water Lily scaffold degraded the fastest (8.5 weeks). These findings provide insights for optimizing scaffold designs for improved mechanical stability and controlled degradation in bone tissue engineering applications. The numerical investigations on impact resistance by Rawat et al.¹⁹⁵ investigated the impact resistance of basalt fiber-reinforced mortar textile composites by comparing three mesh designs: square, diamond, and bioinspired spider web structures. Using FEA, numerical simulations were conducted at impact velocities ranging from 100 to 500 m/s. Results showed that the spider web mesh exhibited superior stretchability and internal energy absorption, preventing fiber failure even at 500 m/s, unlike the square and diamond meshes. The spider web design's unique geometry allowed radial threads to absorb impact forces while spiral threads provided secondary support, enhancing impact resistance. These findings highlight the advantages of bioinspired designs for improving stress distribution and durability in high-velocity impact applications. Amendola et al. 176 also study the discrete-to-continuum approach, which presents composite materials reinforced with spider silk fibers embedded in a matrix. Using the virial stress concept from statistical mechanics, a multiscale FE model was developed to capture the hyperelastic behavior of both the silk fibers and matrix material. Numerical simulations demonstrated that the proposed model effectively replicates the mechanical response of a bare spider orb web and silk composites with weak or elastomeric matrices as shown in Figure 6D. The study provides a robust analytical tool for designing novel bioinspired composites using recombinant or synthetic silk fibers. Future work in this area can incorporate hysteresis effects, strain-rate dependence, and impact loading into the model.

In conclusion, MD simulations have played a pivotal role in uncovering the molecular mechanisms behind spider silk's remarkable mechanical performance, particularly

15512916, 0, Downloaded from https://ceramics.onlinelibrary.wiley.com/doi/10.1111/jace.70241 by Raghavan Ranganathan - Indian Institute of Technology Gandhinagar, Wiley Online Library on [23/09.2025]. See the Terms and Conditions (https://onlinelibrary.wiley.com/terms

and-conditions) on Wiley Online Library for rules of use; OA articles are governed by the applicable Creative Commons License

in bridging the gap between its nanoscale structure and macroscopic properties. In multiple studies, MD has been instrumental in correlating protein-level interactions, especially in β -sheet and amorphous domains, with experimentally observed strength, extensibility, shape memory behavior, and environmental responsiveness. Furthermore, MD simulations measured some key mechanical properties such as elastic modulus, tensile strength, and Gibbs free energy of chain separation, confirming spider silk's exceptional load-bearing capability. Simulations under varied conditions such as electric fields, composite interfaces, and nanoparticle reinforcement have further identified how specific structural motifs or external stimuli alter β -sheet stability, interfacial adhesion, and overall fiber performance. MD models have provided computational efficiency and have been validated against experimental densities and morphologies.

FEM simulations have been based on MD-derived material parameters to simulate larger-scale behaviors, from single threads to full webs, capturing impact resistance, vibration damping, and geometric nonlinearity. Predicted stress-strain curves and fracture patterns match experimental observations and help optimize bioinspired designs. Together, MD and FEM form a multiscale validation loop: MD updates constitutive models, FEM predicts structural performance, and experiments confirm accuracy. This synergy ensures that spider silk's unique molecular-to-macro mechanics are understood and applied in next-generation materials.

BONE

Bone, the principal structural material of the vertebrate skeleton, is a sophisticated composite that masterfully balances strength, stiffness, and toughness to withstand a lifetime of diverse mechanical demands. Beyond its supportive role, bone protects vital organs and provides leverage for movement. 196 The mechanical integrity of bone is crucial for skeletal function and the organism's overall health, as fractures and other bone-related failures can significantly impair the quality of life. The mechanical properties of bone are intimately linked to its hierarchical structure, as shown in Figure 7A, which spans from the nanoscale arrangement of collagen and minerals to the macroscopic architecture of whole bones. 197,198 The primary building blocks are type I collagen fibrils, providing a flexible organic matrix, and hydroxyapatite (HA) crystals, a calcium phosphate mineral that confers rigidity and compressive strength. 199 The arrangement of these components into lamellae, osteons (in cortical bone), and trabeculae (in cancellous bone) creates a complex composite material with anisotropic and heterogeneous

mechanical behavior.²⁰⁰ Cortical bone, the dense outer layer of most bones, exhibits high stiffness and strength, enabling it to resist bending and torsional loads. In contrast, trabecular bone, found in the vertebrae and ends of long bones, has a lower density and higher surface area due to its porous, interconnected structure. ²⁰¹ This architecture provides a high strength-to-weight ratio and effectively absorbs energy during impact. Furthermore, bone is a dynamic tissue that continuously adapts its structure and properties in response to mechanical loading through a process known as bone remodeling.²⁰² This remodeling process, orchestrated by osteoblasts (bone-forming cells) and osteoclasts (bone-resorbing cells), allows the bone to repair microdamage, maintain mineral homeostasis, and optimize its mechanical performance. Understanding the intricate relationship between bone structure, composition, and mechanical properties is essential for preventing and treating osteoporosis, fractures, and other skeletal disorders.²⁰³ Furthermore, the unique combination of mechanical competence and biological compatibility has inspired the development of novel biomaterials for bone regeneration and orthopedic implants. This review will examine the hierarchical organization of bone and its mechanical properties at the atomistic and continuum scales.

6.1 **MD** studies

The study by Fielder and Nair²⁰⁶ used MD simulations to examine how water and mineral content affect the mechanical behavior of collagen fibrils. Fibrils with different mineralization levels (0, 20, and 40 wt%) and hydration (0, 2, and 4 wt%) were tested under tensile stress. The results show that higher hydration increases nonlinearity in stress-strain behavior, while more mineralization reduces this effect. Young's modulus decreases with hydration, and the gap/overlap ratio expands more in nonmineralized fibrils. Water distribution differs based on mineral content, influencing fibril deformation. These findings help in understanding bone mechanics and developing biomimetic tissue materials. Song et al.²⁰⁷ investigated how collagen-ligand interactions enhance intrafibrillar mineralization by cross-linking a negatively charged polyelectrolyte to collagen fibrils. Cryogenic electron microscopy and MD simulations reveal that this cross-linking facilitates the formation of chain-like mineral precursor aggregates, increasing the availability of mineralization precursors. The experimental imaging confirms the structural outcomes predicted by the simulations. Compared to unmodified collagen scaffolds, higherquality mineralized scaffolds with improved biomechanical properties are achieved. The study also suggests that

iournal

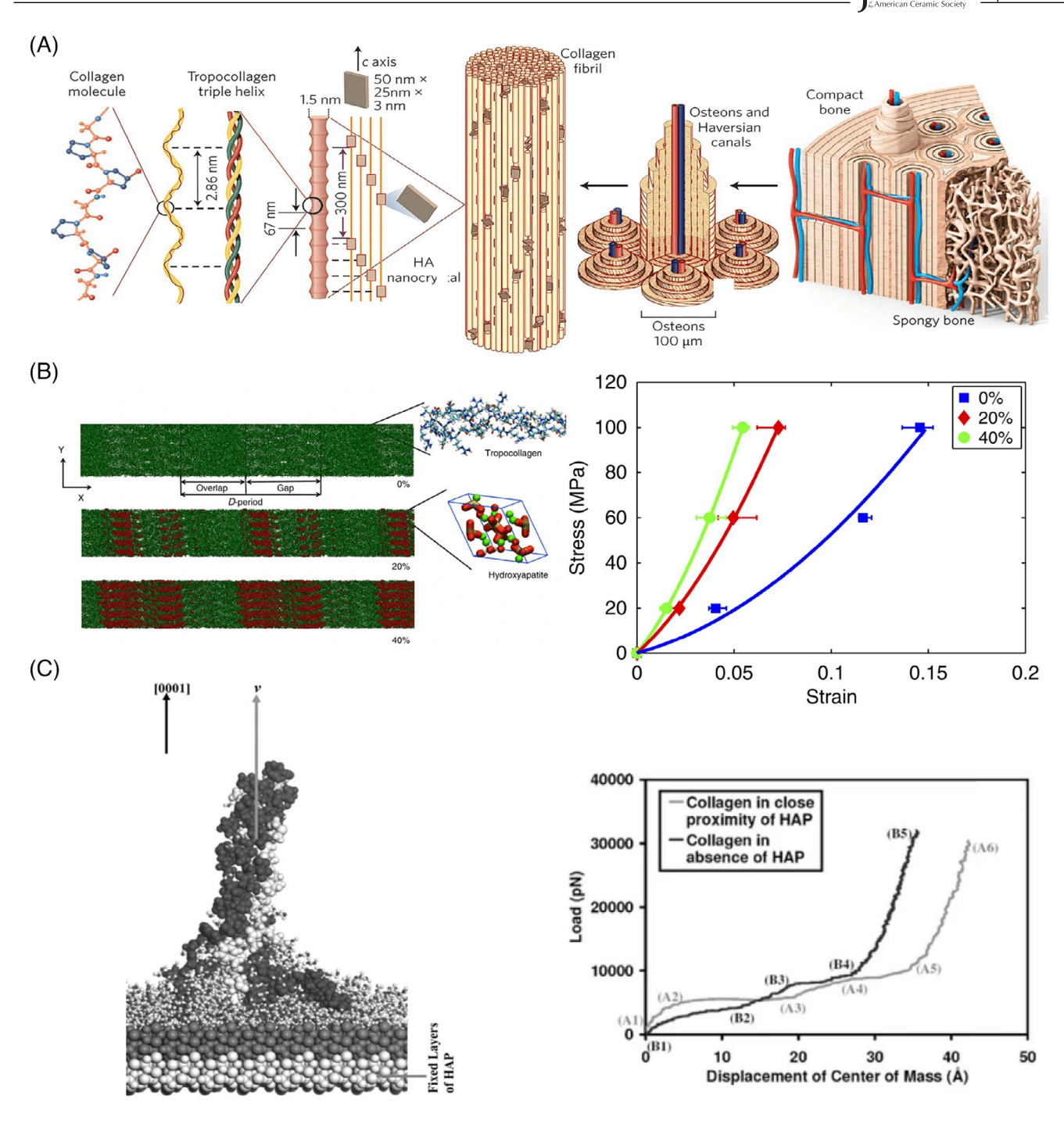


FIGURE 7 (A) The hierarchical structure of cortical bone from macro to nano scale. Reproduced with permissions. ¹⁹⁷ (B) Tensile behavior of bone-like topocollagen (green) and hydroxyapatite (red) composite for varying mineral content through MD simulations. The HA crystals are arranged such that the c-axis of the crystal aligns with the fibril axis. Reproduced with permission from Ref. 204. (C) Pulling of solvated N-Collagen in close proximity to HA and load-displacement curve of solvated collagen molecule in close proximity and in the absence of HA. Reproduced with permission from Ref. 205.

such collagen-ligand interactions could enhance fatigue resistance in biomaterials, making them more suitable for medical applications.

To understand the mechanics of mineralized collagen, Milazzo et al. 208 explored how HA content affects the mechanical properties of mineralized collagen using MD

simulations. Their study modeled collagen fibrils with varying levels of mineralization 0%, 20%, and 40% HA to assess how mineral distribution impacts wave propagation, stiffness, and energy dissipation. The findings showed that stiffness increased by around 80% when HA rose from 0% to 20%, and by another 30% when it

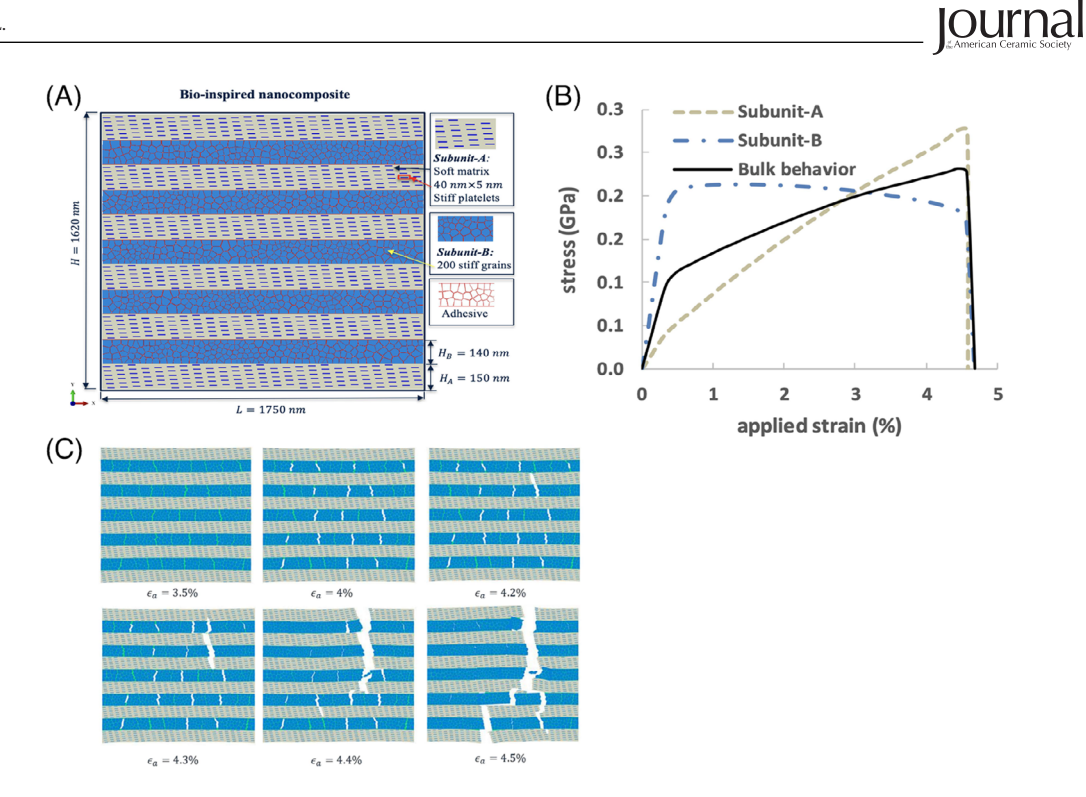
reached 40%. The simulations also indicated that both wave speed and Young's modulus declined at higher loading rates, emphasizing the influence of hydrogen bonding on mechanical performance. Additionally, collagen with 40% HA had an acoustic impedance of about 4×10^6 kgm^2s^{-1} , which is notably lower than bone's 7.5×10^6 kgm^2s^{-1} likely due to the absence of extra-fibrillar mineralization. A similar study was done by Nair et al²⁰⁴ as shown in Figure 7B. Furthermore, Tavakol and Vaughan²⁰⁹ examined the mechanical behavior of mineralized collagen fibrils (MCFs) using a CGMD approach. Their study focused on how the amount and arrangement of minerals affect the fibrils' mechanical performance. They found that the mineral phase plays a key role in restricting collagen sliding, which significantly boosts the UTS. While mineralized protofibrils primarily carry the load, the nonmineralized ones help redirect cracks, enhancing damage resistance. The simulations shed light on how stress is distributed within the structure, revealing both tensile and shear stress responses. Their results showed that as mineral content increases, so do work-hardening, UTS, and overall toughness, supported by clear trends in the stress-strain curves. Alcantara et al.²¹⁰ explored how the extrafibrillar volume (EFV) affects the mechanical properties of mineralized bone microfibrils using fully atomistic MD simulations. Their models included type-I collagen, HA, and water, capturing mineral content in both the EFV and intrafibrillar volume. The study looked at how varying degrees of mineralization impact structural and elastic behavior, showing that EFV plays a major role by carrying higher stress. As mineral content increased, bone stiffness also improved, with Young's modulus rising from around 6.22 to 14.45 GPa based on the level of mineralization. The study highlights the importance of EFV in bone biomechanics and suggests its crucial role in load-bearing capacity. MD simulations provided insights into nanoscale stress distribution, revealing that HA in EFV bears most of the load, which is vital for understanding bone mechanics and disease-related fragility. Similarly, Bhowmik et al.²⁰⁵ studied the interface between HA with collagen molecule as shown in Figure 7C.

6.2 **FEM studies**

The study by Frank et al. 211 investigated the effect of hydration on the mechanical properties of trabecular bone using micro-tensile tests and MD simulations. Results show that dehydration increases Young's modulus, yield stress, and ultimate stress approximately twofold but reduces failure strain and post-yield work, leading to brittle failure. In contrast, hydrated samples exhibit ductile failure with a larger area of microdamage accumulation. The

findings highlight the importance of maintaining physiological conditions during mechanical testing. Moreover, to understand more about elastic constants in a lamellar bone, Martinez et al. 212 developed explicit expressions to estimate the transversely isotropic elastic constants of lamellar bone based on bone mineral density (BMD). Using FE analysis, homogenization techniques, and continuum mechanics, the study quantified how BMD influences the elastic modulus, shear stiffness, and poisson's ratios of lamellar bone. Results show that while BMD significantly affects elastic properties, the fibril orientation pattern primarily governs the anisotropic behavior of cortical bone. The study also models cortical bone porosity, highlighting its impact on mechanical properties. These findings improve bone fracture risk assessment and provide a foundation for modeling osteoporosis-related porosity effects in future research. Similarly, to study the cortical bone fracture, Wang and Ural²¹³ developed a novel 3D modeling approach to investigate the fracture behavior of MCF networks in cortical bone at the submicroscale. The study used FE analysis to examine how MCF size and orientation influence damage mechanisms under transverse and longitudinal loading. Results showed that transverse loading primarily led to fibril separation, while longitudinal loading caused fibril rupture. The mechanical properties increased with fibril misalignment under transverse loading but decreased under longitudinal loading. Fracture energy was significantly higher in longitudinal loading, and larger MCF diameters improved mechanical properties in transverse loading. To study how modifications in MCF and extra-fibrillar matrix (EFM) affect bone mechanics at the microscale, they²¹⁴ developed a 3D FEM model to simulate tensile loading in different orientations, evaluating elastic modulus, ultimate strength, and fracture resistance. The study demonstrated how material modifications can affect the fracture resistance mechanism of fibril rupture and separation. Moreover, they also²¹⁵ studied elastic modulus, ultimate strength, and fracture energy under longitudinal (MCF rupture) and transverse (MCF separation) tensile loading. Results showed that mineral uniformity and stronger MCF interactions enhanced mechanical properties under longitudinal loading, whereas only MCF interactions influenced transverse loading. Mechanical properties exhibited exponential variation with mineral distribution, while full mineralization led to only a modest increase in strength.

Traditional experimental approaches using cadaveric and synthetic bones have limitations, particularly in capturing long fracture paths; Marco et al.216 analyze different numerical modeling techniques for predicting femur fracture morphology using FEM. The researchers compared various numerical methods and validated them



(A) A bone-inspired hybrid composite features alternating parallel subunits A and B, joined by a thin adhesive layer. Subunit A mimics mineralized collagen fibrils, and subunit B represents the extrafibrillar matrix. (B) Stress-strain relation of bulk composite and its basic subunits. (C) During deformation, subunit B develops multiple cracks in the post-yield stage, enabling energy dissipation and influencing the composite's stress-strain behavior. Reproduced with permission from Ref. 217.

against experimental results. It was identified that simulating crack growth through incremental material property degradation provides the most accurate and stable results, effectively predicting long crack paths without convergence issues. This method was successfully applied to real human femurs, accurately replicating intracapsular and extracapsular fractures.

There are several studies by Ganjeh et al., wherein they²¹⁷ developed a two-dimensional cohesive FE model to investigate the mechanical behavior of bone at the sublamellar level, bridging the nano- and microscale hierarchies. The model considers bone as a composite of MCFs embedded in an EFM composed of HA polycrystals and noncollagenous proteins. Simulations under tensile and compressive loading revealed that EFM primarily governs pre-yield deformation, while failure mechanisms vary by loading mode—nanocracks form in tension, while shear bands and delamination occur in compression, as shown in Figures 8A–C. Moreover, they also²¹⁸ use the cohesive FE method to model a 3D hybrid nanocomposite that mimics the ultrastructure of bone and nacre. The model consists of mineral nanograins bonded by a thin organic adhesive layer, which enhances toughness through cohesive damage, nanocrack formation, and complex crack trajectories. Simulations revealed strain-hardening and strain-softening behaviors, highlighting the necessity of 3D modeling. Numerical results showed an elastic modu-

lus of 25 GPa, ultimate stress of 160 MPa, and failure strain of 1.3%, closely matching bone properties (E = 18.2 GPa, ultimate stress = 92.95 MPa). The post-yield strain hardening was attributed to distributed damage and energy dissipation in the organic phase, while strain softening was linked to nanocracking and fracture deviations. FE analysis was crucial in capturing the mechanical behavior, demonstrating how the organic interface significantly influences the nanocomposite's bulk response despite its small volume fraction. Moreover, to know how bound water influences the mechanical behavior of bone at the ultrastructural level, Ganjeh et al.²¹⁹ built a 2D cohesive FE model, wherein the model incorporates MCFs, EFM, and their interfaces to simulate hydrated and dehydrated conditions. Numerical results show that the energy dissipation in hydrated bone ($\approx 7 \times 10^{-7}$ J) is nearly 10 times greater than in dehydrated bone ($\approx 7 \times 10^{-8}$ J). The elastic modulus of wet bone was found to be 18 GPa, significantly lower than the 53 GPa predicted by the rule-of-mixtures due to the influence of softer non-collagenous proteins in EFM. Additionally, the stress in intrafibrillar mineral platelets is much higher in dry bone (≈115 MPa) compared to wet bone (\approx 20 MPa), contributing to the brittle nature of dehydrated bone. The study suggests hydration weakens but toughens bone by promoting energy dissipation mechanisms, such as nanocrack formation, debonding, and crack bridging. In contrast, dehydration strengthens

15512916, 0, Downloaded from https://ceramics.onlielibrary.wiley.com/doi/10.1111/jace.70241 by Raghavan Ranganathan - Indian Institute of Technology Gandhiragar , Wiley Online Library on [23/9/02025]. See the Terms and Conditions (https://onlinelibrary.wiley.com/terms

and-conditions) on Wiley Online Library for rules of use; OA articles are governed by the applicable Creative Commons License

the interfaces, making bone stiffer and stronger but more brittle by reducing these mechanisms.

The Haversian bone architecture for enhanced energy absorption and crashworthiness was studied by Nikkhah et al.²²⁰, wherein they developed and analyzed a total of 18 nested tube designs with circular, hexagonal, and square cross-sections, both with and without reinforcement walls. The results revealed three deformation stages, with reinforcement walls significantly improving energy absorption. The nested tube with reinforcement walls (S-H-Cr) demonstrated the best performance, offering the highest specific energy absorption and lower impact force. This configuration was identified as the optimal design using the multicriteria decision-making method. Validated by quasi-static experimental tests, FE simulations were used to study their crashworthiness and progressive deformation behavior. Moreover, Wang et al.²²¹ introduced a bioinspired crash box design, modeled after the human tibia, to enhance crashworthiness and energy absorption. The novel structure consists of a concave outer shell and a functionally graded inner core made of negative Poisson's ratio material, mimicking the cancellous bone structure. FEM was used to simulate crash scenarios and evaluate the performance of different design variables, such as shell thickness and inner core gradient. Multiobjective optimization using response surface methodology and Latin hypercube design was conducted with AMGA and NSGA-II algorithms. The NSGA-II-optimized design significantly improved energy absorption and crash stability, making the collision process more controlled. Adding to this, Salem et al.²²² developed an equivalent constitutive model. Using microscale XFEM models in ABAQUS, the study replicated cancellous bone's mechanical response and translated these behaviors into a macroscale model. The analysis shows that cancellous bone exhibits orthotropic behavior, with higher strength and failure strain in compression than in tension. The FEM study confirms that the cast iron plasticity model effectively replicates cancellous bone mechanics without modeling individual trabeculae, significantly reducing computational costs while maintaining accuracy. Numerical results in 3D indicate Young's modulus values of 2.05, 3.7, and 5.7 GPa for the X, Y, and Z anatomical directions, respectively, with ultimate strengths ranging from 7.2 to 21.3 MPa. The study also demonstrates that XFEM predicts fractures more effectively than traditional FEM, providing valuable insights into bone mechanics.

The study by Belda et al.²²³ investigated cancellous bone fracture under quasi-static compression using micro-CT-based finite element modeling and digital image correlation on 13 specimens. High-resolution imaging enabled detailed strain analysis, revealing that equivalent strain best predicts fracture patterns, with a consistent yield

strain of 0.0068 and variable fracture strain across specimens. Micro-FE models provided more accurate fracture predictions than DIC, which underestimated peak strain by 10-24%, and highlighted that segmentation accuracy greatly impacts Young's modulus estimation. The study by Demirtas and Ural²²⁴ investigated the impact of microcracks and tissue compositional heterogeneity on the fracture resistance of human cortical bone, wherein compact tension specimen tests were simulated with varying microcrack density, location, clustering, and material heterogeneity across three different bone samples. The results revealed that higher microcrack density improved fracture resistance, but reduced material heterogeneity weakened bone strength. When both changes were combined (as in bisphosphonate-treated bone), fracture resistance decreased, supporting the hypothesis that loss of compositional heterogeneity is a key factor in bone fragility. Using XFEM, Marco et al.²²⁵ developed a phantom node method in Abaqus with a new crack orientation criterion to accurately model crack growth in the cortical bone at the microstructural level. This approach accounts for bone heterogeneity, unlike standard XFEM, which fails to capture cracks propagating along cement lines. FEM validated the model using LEFM tests, achieving 1% error in stress intensity factor estimation. The model successfully predicted crack paths along cement lines, aligning with experimental data and demonstrating its potential for modeling fracture in other heterogeneous materials.

Gustafsson et al.²²⁶ carried out a parametric study of 14 material factors using XFEM and found that interface strength and stiffness significantly impact crack deflection, while matrix and osteon stiffness had little effect. Lower interface stiffness enhanced deflection, while reduced matrix toughness increased crack penetration, highlighting aging-related fracture risks. XFEM enabled realistic crack path predictions, showing that cement line properties affect fracture energy dissipation, not crack trajectory. Moreover, they also²²⁷ developed a 2D crack propagation model to analyze how microstructural features, particularly cement line strength and Haversian canals, influence fracture resistance. The model combined the maximum principal strain criterion with an interface damage formulation, allowing it to accurately capture crack deflections at osteon boundaries, as observed experimentally. Results showed that weak cement lines caused cracks to deflect along osteon boundaries, while strong cement lines led to crack penetration through osteons. Additionally, Haversian canals weakened the structure, especially in the longitudinal orientation. Lamellar bone is a type of wellorganized bone tissue found in cortical and trabecular bone. Razi et al.²²⁸ analyzed crack propagation in lamellar bone, focusing on how periodic variations in mechanical properties enhance strength and fracture toughness. The

model simulated a heterogeneous lamellar structure and showed that microcracks form ahead of the main crack tip, dissipating energy and improving toughness without further crack propagation. Compared to a homogeneous material with the same average properties, the lamellar structure exhibited higher strength and toughness due to reduced crack-driving forces. The microcrack length corresponded to lamella thickness, confirming that damage tolerance in bone arises from controlled imperfections.

In summary, MD studies are primarily employed to investigate nanoscale mechanisms in bone-like structures, with a central focus on interfacial interactions and the dynamics of protein–mineral components. Specifically, MD helps model the interaction between collagen and HA phases, revealing how the nature of bonding such as hydrogen and ionic bonds affects load transfer and failure initiation. The effect of hydration, crosslinking, and HA content and their arrangement in the microstructure have been widely studied through MD. These studies have shown that hydration generally improves the toughness of bone, while crosslinking contributes to increased fracture resistance. Additionally, optimizing the HA content in bone-like materials can lead to improved combinations of stiffness and toughness.

FEM has been extensively employed to investigate the micromechanical behavior of bone-like materials. These studies have primarily focused on simulating the mechanical response of trabecular and cortical bone, as well as bioinspired structures featuring gradient porosity or layered architectures. A key finding across these investigations is the pronounced anisotropy of bone-like materials, which often results in orthotropic mechanical behavior and direction-dependent failure mechanisms. Additionally, the effects of hydration, microstructural variations, and other factors have been analyzed to understand both the quasi-static and dynamic mechanical responses of these composites.

Given the hierarchical architecture of bone that spans from nanoscale to macroscale, the integration of MD and FEM can prove to be a powerful technique to capture phenomena scaling nano to continuum scale. In this integrated approach, quantitative data extracted from MD such as elastic moduli, fracture toughness, and interface strength can be used to form material constitutive models for FEM frameworks, facilitating accurate simulation of more complex geometries and loading conditions.

7 | SUMMARY

Biomimetics draws inspiration from nature's hierarchical designs to develop materials with superior mechanical properties and multifunctional capabilities. Computa-

tional tools like MD and FEM have proven invaluable in uncovering the structure-property relationships of such materials across different length and time scales. FEM models allow multiscale translation of these mechanisms, enabling macroscopic predictions of stress distribution, crack propagation, and structural resilience, while MD simulations offer insight into atomic-scale interactions that directly influence the deformation mechanisms and fundamental mechanical behavior of the material system. Natural materials such as nacre, mantis shrimp appendages, spider silk, and bone have been explored using these tools to develop synthetic analogs with superior mechanical response. These insights are increasingly being applied in protective gear, aerospace components, biomedical scaffolds, and lightweight structural materials, where energy absorption, toughness, and durability are critical. A summary of the computational studies of bioinspired microstructures covered in this review, along with their key implications, is provided in Table 1.

8 | CHALLENGES, OUTLOOK, AND SCOPE FOR FUTURE WORK

Developing new materials using traditional experimental techniques has been a very slow and labor-intensive task. Computational methods such as DFT, MD, and FEM with additive manufacturing (AM) are significantly faster and more cost-effective alternatives to experiments; still, the length and time-scale challenges associated with them limit their applicability across various fields, including in biomimetic materials design. ^{229,230} Abstracting the complex mineralization process of nature, for the development of state-of-the-art high-performance materials, has traditionally been a challenge, which has partly been overcome over the past few decades thanks to advancements in theoretical understanding of these processes and structures.

8.1 | Artificial intelligence/machine learning for material design and discovery

A large effort has been made in the last decade to employ artificial intelligence (AI) andmachine learning (ML)-based techniques to accelerate material design and discovery. Most of the ML techniques can be categorized into four categories: probability estimation, regression, classification, and clustering. These techniques require large datasets on which a model can be trained, followed by model evaluation, which can then be used to make precise property predictions. The datasets can be generated using quantum mechanical calculations or obtained from various open-source databases available in the material science

TABLE 1 Summary of computational studies of bioinspired structures and their implications.

Microstructure	Important implications
Nacre	 The strength, modulus, and toughness of nacre and nacre-inspired composites are primarily influenced by the filler content, the physical and chemical interactions between constituent phases, polymer nanoconfinement and geometrical parameters, especially the tablet aspect ratio and the overlap length between adjacent tablets. ^{70,111} Interfacial modifications, such as filler alignment, high hard-phase content, reinforcement with bridges, and ternary structure, have been found to enhance the mechanical properties of 3D bulk nacre-like composites. ^{80,81} Nacre-like composites have demonstrated improved mechanical performance under both quasi-static and dynamic loading conditions, including impact, when their microstructures exhibit optimal tablet size and overlap. ^{72,117}. Surface characteristics of filler materials, including waviness, roughness, and chemical functionalization, enhance the strength and toughness of brick-and-mortar composites in a manner analogous to the role of asperities and mineral bridges in natural nacre. ^{93,118}
Dactyl club	 Best impact resistance at small pitch angles (18°-42°); reduced interfacial adhesion = better energy dissipation.¹³⁵ Increasing crosslink density between CNTs enhances energy dissipation.¹³⁸ Compared to cross-ply laminates, helicoidal laminates delay failure and achieve 30% higher peak load due to a single large mid-plane delamination.¹⁴³ Varying fiber orientations (0°, 90°): 0° blocks crack; 90° promotes crack.¹⁵⁸
Spider silk	 eMaSp2 fibers showed excellent shape memory behavior with 98.5% recovery and high recovery stress of 18.5 MPa.¹⁷⁷ spider web energy dissipation is governed by silk microstructure for small prey and aerodynamic drag for larger impacts.¹⁸⁶ Tensegrity and multiscale FEM models capture crack-stopping and fracture toughness.¹⁸⁸ Stiffening via chain density; flexibility via Kuhn number; accurate stress-strain prediction.¹⁸⁹
Bone	 Higher hydration increases stress-strain nonlinearity; higher mineralization reduces it.²⁰⁶ Collagen-ligand cross-linking improves mineralization and enhances the fatigue resistance in bio-materials.²⁰⁷ In mineralization levels of HA, 0% → 20% HA leads to 80% increase in stiffness; 20% → 40% HA adds 30% more.²⁰⁸ The mineral phase limits collagen sliding, contributing significantly to ultimate tensile strength in mineralized collagen fiber.²⁰⁹

community, like AFLOW,^{231,232} Materials Project,^{233–235} ICSD,²³⁶ OQMD,^{237,238} JARVIS-DFT,^{239,240} NOMAD,^{241,242} and Organic Materials DB.²⁴³ Some of the widely used ML algorithms in the material science community include linear and logistic regression, support vector machines, neural networks, decision trees, random Forest, extreme gradient boosting, K-means clustering, generative AI, and several others.

The advancement in AI and ML has revolutionized the field of bioinspired materials by designing materials with customized properties for various applications. With AI and ML, millions of test cases can be analyzed rapidly, which can reduce the time and cost for design space exploration. An ML model can learn the relationship between material features and its mechanical behavior using geometric configurations as inputs, without explicitly considering the physical laws, like in a typical MD technique. Several ML techniques like artificial neural network, single and multilayer perceptrons, convolution neural networks, decision trees, generative AI models like gener-

ative adversarial network (GAN), large language models (LLM) and genetic algorithms have been successfully used to predict material strength and toughness, 244-246 elastic modulus,²⁴⁷ superhydrophobic behavior,²⁴⁸ as well as in the design of composites and bioinspired ceramics materials, ^{249,250} and the development of complex architected structures. 251,252 Emergence of advanced generative models like GAN and transfer models has accelerated the development of materials with tailored properties by learning through the complex hierarchical patterns found in the natural materials. It is now successfully used in the field of biomimetic materials to design, optimize, and predict mechanical properties such as elasticity, strength, and toughness, and to create complex and hierarchical porous structures with controlled pore size and geometry. 253,254 Although, while training generative AI models, the type and quality of the data play a crucial role, and it should come from trusted and relevant sources. The diversity across different datasets is also important for the model to learn from a broad spectrum of patterns and produce

onlinelibrary. wiley.com/doi/10.1111/jace.70241 by Raghavan Ranganathan - Indian Institute of Technology Gandhinagar, Wiley Online Library on [23/09/2025]. See the Terms and Conditions (https://onlinelibrary.wiley.

und-conditions) on Wiley Online Library for rules of use; OA articles are governed by the applicable Creative Commons License

accurate and reliable results. In addition, the integration of generative AI particularly LLMs featuring natural language processing capabilities, with AM, has been useful in process parameter optimization, thereby enhancing the efficiency of and productivity of the manufacturing processes. 254,255

8.2 | Additive manufacturing, FEM, and MD: A combined approach

The FEM provides indispensable insights into the characteristics that lead to stress distribution and structural deformations at the macroscopic level in composite materials. Complementing FEM, atomic-level interactions that govern a material's strength and toughness can be understood by employing MD methods. In the experimental realm, AM in particular, has been very useful in mimicking the multiscale, multimaterial, and multifunctional aspects of the complex nature-inspired structures that are difficult to process with traditional design and fabrication technologies.²⁵⁶ Some of the recent studies using the combined approaches include nacre and bouligand-inspired composites of alumina with carbon fiber reinforcement, 141,257 nacre-based cement-epoxy resin and graphene/silicate composites, 258,259 tooth enamelbased biomimetic composites, ²⁶⁰ mussel-inspired soybean protein adhesives, ²⁶¹ triply periodic minimal surface scaffold inspired by the dactyl club,²⁶² among many others. In all these studies, FEM was helpful in predicting the stress and strain distribution through the material and its effect on the fracture characteristics and crack propagation behavior during the material fracture. MD provided insight into the local structure and bond breaking and formation mechanism at the interface, which affect material ductility and toughness, including the atomic origin of the deformation mechanism and mechanical behavior in the systems. This combined multiscale approach bridges the gap between atomic-level interactions and macroscale mechanical behaviors of composite materials. Understanding the atomic-level mechanism that governs the macroscale behavior could be useful in designing new materials with tailored properties. In addition, with the integration of additive manufacturing, the capability to physically fabricate these geometrically complex materials with customized and tailored properties for particular purposes becomes feasible. Future research holds immense promise in the abstraction of the complex processing—structure-property relationships and realization of hierarchical biomimetics possessing enhanced properties through rational design, with the aid of computational studies.

ACKNOWLEDGMENTS

The authors have nothing to report.

ORCID

Raghavan Ranganathan https://orcid.org/0000-0003-1015-791X

REFERENCES

- 1. Fratzl P. Biomimetic materials research: what can we really learn from nature's structural materials? J R Soc Interface. 2007:4:637-42.
- 2. Naik RR, Singamaneni S. Introduction: bioinspired and biomimetic materials. ACS Publications; 2017.
- 3. Yan X, Bethers B, Chen H, Xiao S, Lin S, Tran B, et al. Recent advancements in biomimetic 3D printing materials with enhanced mechanical properties. Front Mater. 2021;8:518886.
- 4. Zhang Y, Li X. Bioinspired, graphene/Al2O3 doubly reinforced aluminum composites with high strength and toughness. Nano Lett. 2017;17:6907-15.
- 5. Sandak A, Butina Ogorelec K. Bioinspired building materialslessons from nature. Front Mater. 2023;10:1283163.
- 6. Montero de Espinosa L, Meesorn W, Moatsou D, Weder C. Bioinspired polymer systems with stimuli-responsive mechanical properties. Chem Rev. 2017;117:12851-92.
- 7. Lazarus BS, Velasco-Hogan A, Gómez-del Río T, Meyers MA, Jasiuk I. A review of impact resistant biological and bioinspired materials and structures. J Mater Res Technol. 2020;9:15705-38.
- 8. Wang R, Suo Z, Evans A, Yao N, Aksay IA. Deformation mechanisms in nacre. J Mater Res. 2001;16:2485-93.
- 9. Meo M, Rizzo F, Portus M, Pinto F. Bioinspired helicoidal composite structure featuring functionally graded variable ply pitch. Materials. 2021;14:5133.
- 10. Huemmerich D, Scheibel T, Vollrath F, Cohen S, Gat U, Ittah S. Novel assembly properties of recombinant spider dragline silk proteins. Cur Biol. 2004;14:2070-4.
- 11. Rosa N, Moura MF, Olhero S, Simoes R, Magalhães FD, Marques AT, et al. Bone: an outstanding composite material. Appl Sci. 2022;12:3381.
- 12. Huang C, Peng J, Cheng Y, Zhao Q, Du Y, Dou S, et al. Ultratough nacre-inspired epoxy-graphene composites with shape memory properties. J Mater Chem A. 2019;7:2787-94.
- 13. Liu J, Li S, Fox K, Tran P. 3D concrete printing of bioinspired Bouligand structure: a study on impact resistance. Addit Manuf. 2022;50:102544.
- 14. Chappard D, Baslé MF, Legrand E, Audran M. New laboratory tools in the assessment of bone quality. Osteop Int. 2011;22:2225-40.
- 15. Yaraghi NA, Guarín-Zapata N, Grunenfelder LK, Hintsala E, Bhowmick S, Hiller JM, et al. A sinusoidally-architected helicoidal biocomposite. arXiv preprint arXiv:160407798. 2016.
- 16. Wu D, Koscic A, Schneider S, Dubini RC, Rodriguez Camargo DC, Schneider S, et al. Unveiling the dynamic self-assembly of a recombinant dragline-silk-mimicking protein. Biomacromolecules. 2024;25:1759-74.
- 17. Manno R, Gao W, Benedetti I. Engineering the crack path in lattice cellular materials through bio-inspired micro-structural alterations. Extreme Mech Lett. 2019;26:8-17.

18. Libonati F. Buehler MJ. Advanced structural materials by bioinspiration. Adv Eng Mater. 2017;19:1600787.

journal

- 19. Ural A. Advanced modeling methods-applications to bone fracture mechanics. Cur Osteop Rep. 2020;18:568-76.
- 20. Kolednik O, Predan J, Fischer FD, Fratzl P. Bioinspired design criteria for damage-resistant materials with periodically varying microstructure. Adv Funct Mater. 2011;21:3634-41.
- 21. Dao VD, Nguyen HTK. Nature-inspired design for highefficiency solar-driven water evaporation. J Power Sources. 2024:609:234676.
- 22. Frenkel D, Smit B. Understanding molecular simulation. San Diego, CA: Academic Press: 2002.
- 23. Wang S, Sun Q, Zhang Q, Li C, Xu C, Ma Y, et al. Li-ion transfer mechanism of ambient-temperature solid polymer electrolyte toward lithium metal battery. Adv Energy Mater. 2023;13:2204036.
- 24. Jeon I, Yun T, Yang S. Classical, coarse-grained, and reactive molecular dynamics simulations on polymer nanocomposites. Multiscale Sci Eng. 2022;4:161-78.
- 25. Rahman A, Saikia B, Gogoi CR, Baruah A. Advances in the understanding of protein misfolding and aggregation through molecular dynamics simulation. Prog Biophys Mol Biol. 2022;175:31-48.
- 26. Majidi S, Erfan-Niya H, Azamat J, Ziaei S, Cruz-Chú ER, Walther JH. Membrane based water treatment: insight from molecular dynamics simulations. Sep Purif Rev. 2023;52:336-52.
- 27. Senftle TP, Hong S, Islam MM, Kylasa SB, Zheng Y, Shin YK, et al. The ReaxFF reactive force-field: development, applications and future directions. npj Comput Mater. 2016;2:
- 28. Mabrouk Y, Safaei N, Hanke F, Carlsson J, Diddens D, Heuer A. Reactive molecular dynamics simulations of lithium-ion battery electrolyte degradation. Sci Rep. 2024;14:10281.
- 29. Chenoweth K, Van Duin AC, Goddard WA. ReaxFF reactive force field for molecular dynamics simulations of hydrocarbon oxidation. J Phys Chem A. 2008;112:1040-53.
- 30. Nyden MR, Stoliarov SI, Westmoreland PR, Guo Z, Jee C. Applications of reactive molecular dynamics to the study of the thermal decomposition of polymers and nanoscale structures. Mater Sci Eng, A. 2004;365:114-21.
- 31. Mao Q, Feng M, Jiang XZ, Ren Y, Luo KH, van Duin AC. Classical and reactive molecular dynamics: principles and applications in combustion and energy systems. Prog Energy Combust Sci. 2023;97:101084.
- 32. Neri M, Anselmi C, Cascella M, Maritan A, Carloni P. Coarsegrained model of proteins incorporating atomistic detail of the active site. Phys Rev Lett. 2005;95:218102.
- 33. Bereau T, Deserno M. Generic coarse-grained model for protein folding and aggregation. Biophys J. 2009;96:405a.
- 34. Marrink SJ, De Vries AH, Mark AE. Coarse grained model for semiquantitative lipid simulations. J Phys Chem B. 2004:108:750-60.
- 35. West B, Brown FL, Schmid F. Membrane-protein interactions in a generic coarse-grained model for lipid bilayers. Biophys J. 2009;96:101-15.
- 36. Akkermans RL, Briels WJ. A structure-based coarse-grained model for polymer melts. J Chem Phys. 2001;114:1020-31.

- 37. Arash B. Park HS, Rabczuk T. Mechanical properties of carbon nanotube reinforced polymer nanocomposites: a coarsegrained model. Compos Part B: Eng. 2015;80:92-100.
- 38. Arash B. Park HS. Rabczuk T. Tensile fracture behavior of short carbon nanotube reinforced polymer composites: a coarse-grained model. Compos Struct. 2015;134:981-8.
- 39. Dürholt JP, Galvelis R, Schmid R. Coarse graining of force fields for metal-organic frameworks. Dalton Trans. 2016:45:4370-9.
- 40. Bathe KJ, Wilson E. Numerical methods in finite element analysis, 1976.
- 41. Ramakrishnan N, Arunachalam V. Finite element methods for materials modelling. Prog Mater Sci. 1997;42:253-61.
- 42. Sabat L, Kundu CK. History of finite element method: a review. Recent Developments in Sustainable Infrastructure: Select Proceedings of ICRDSI 2019. 2020:395-404.
- 43. Liu WK, Li S, Park HS. Eighty years of the finite element method: birth, evolution, and future. Arch Comput Methods Eng. 2022;29:4431-53.
- 44. Phellan R, Hachem B, Clin J, Mac-Thiong JM, Duong L. Real-time biomechanics using the finite element method and machine learning: review and perspective. Med Phys. 2021;48:7-18.
- 45. Civalek Ö, Uzun B, Yaylı MÖ, Akgöz B. Size-dependent transverse and longitudinal vibrations of embedded carbon and silica carbide nanotubes by nonlocal finite element method. Eur Phys J Plus. 2020;135:381.
- 46. Guo Q, Yao W, Li W, Gupta N. Constitutive models for the structural analysis of composite materials for the finite element analysis: a review of recent practices. Compos Struct. 2021;260:113267.
- 47. Jahanbakhshi A, Heidarbeigi K. Simulation and mechanical stress analysis of the lower link arm of a tractor using finite element method. J Fail Anal Prev. 2019;19:1666-72.
- 48. Belhocine A, Abdullah OI. Thermomechanical model for the analysis of disc brake using the finite element method in frictional contact. Multiscale Sci Eng. 2020;2:27-41.
- 49. John V. Finite element methods for incompressible flow problems. vol. 51. Springer; 2016.
- 50. Pepper DW, Heinrich JC. The intermediate finite element method: fluid flow and heat transfer applications. Routledge; 2017.
- 51. Polycarpou AC. Introduction to the finite element method in electromagnetics. Springer Nature; 2022.
- 52. Burlayenko V, Altenbach H, Sadowski T, Dimitrova S, Bhaskar A. Modelling functionally graded materials in heat transfer and thermal stress analysis by means of graded finite elements. Appl Math Modell. 2017;45:422-38.
- 53. Huang Y, Yang L, Du X, Yang Y. Finite element analysis of thermal behavior of metal powder during selective laser melting. Int J Therm Sci. 2016;104:146-57.
- 54. Nithiarasu P, Lewis RW, Seetharamu KN. Fundamentals of the finite element method for heat and mass transfer. John Wiley
- 55. Dobrzański L, Pusz A, Nowak A, Górniak M. Application of FEM for solving various issues in material engineering. Simulation. 2010;16:26.
- 56. Erhunmwun ID, Ikponmwosa U. Review on finite element method. J Appl Sci Environ Manage. 2017;21:999-1002.

- Barthelat F. Biomimetics for next generation materials. Philos Trans R Soc London, Ser A. 2007;365:2907–19.
- 58. Fleischli FD, Dietiker M, Borgia C, Spolenak R. The influence of internal length scales on mechanical properties in natural nanocomposites: a comparative study on inner layers of seashells. Acta Biomater. 2008;4:1694–706.
- Jackson A, Vincent JF, Turner R. The mechanical design of nacre. Proc Roy Soc Lond Ser B Biol Sci. 1988;234:415– 40.
- Sarikaya M, Gunnison K, Yasrebi M, Aksay I. Mechanical property-microstructural relationships in abalone shell. MRS Online Proc Library. 1989;174:109–16.
- Bourrat X, Francke L, Lopez E, Rousseau M, Stempflé P, Angellier M, et al. Nacre biocrystal thermal behaviour. CrystengComm. 2007;9:1205–8.
- 62. Sun J, Bhushan B. Hierarchical structure and mechanical properties of nacre: a review. RSC Adv. 2012;2:7617–32.
- 63. Checa AG, Cartwright JH, Willinger MG. Mineral bridges in nacre. J Struct Biol. 2011;176:330–9.
- Evans A, Suo Z, Wang R, Aksay IA, He M, Hutchinson J. Model for the robust mechanical behavior of nacre. J Mater Res. 2001;16:2475–84.
- Katti KS, Katti DR, Pradhan SM, Bhosle A. Platelet interlocks are the key to toughness and strength in nacre. J Mater Res. 2005;20:1097–100.
- 66. Liang S, Ji H, Li X. The crucial role of platelet stacking mode in strength and toughness of nacre. Mater Des. 2023;230:111987.
- Yourdkhani M, Pasini D, Barthelat F. Multiscale mechanics and optimization of gastropod shells. J Bionic Eng. 2011;8:357– 68
- 68. Barthelat F, Tang H, Zavattieri PD, Li CM, Espinosa HD. On the mechanics of mother-of-pearl: a key feature in the material hierarchical structure. J Mech Phys Solids. 2007;55:306–37.
- 69. Bourrat X, Rousseau M, Lopez E, Stempflé P. Nano-composite structure of nacre biocrystal. In: BioMin 2005, 9th International Symposium on Biomineralization. BioMin; 2005. p. 6p.
- 70. Shao C, Keten S. Stiffness enhancement in nacre-inspired nanocomposites due to nanoconfinement. Sci Rep. 2015;5:16452.
- Xia W, Song J, Meng Z, Shao C, Keten S. Designing multi-layer graphene-based assemblies for enhanced toughness in nacreinspired nanocomposites. Mol Syst Des Eng. 2016;1:40–7.
- 72. Singh PP, Ranganathan R. Superior impact resistance conferred by hierarchical nacre-inspired nanocomposites: a molecular dynamics study. Carbon. 2025;233:119885.
- 73. Currey JD. Mechanical properties of mother of pearl in tension. Proc R Soc Lond Ser B Biol Sci. 1977;196:443–63.
- Menig R, Meyers M, Meyers M, Vecchio K. Quasi-static and dynamic mechanical response of Haliotis rufescens (abalone) shells. Acta Mater. 2000;48:2383–98.
- 75. Barthelat F, Espinosa H. An experimental investigation of deformation and fracture of nacre–mother of pearl. Exp Mech. 2007;47:311–24.
- Smith BL, Schäffer TE, Viani M, Thompson JB, Frederick NA, Kindt J, et al. Molecular mechanistic origin of the toughness of natural adhesives, fibres and composites. Nature. 1999;399:761– 3
- 77. Zhang N, Chen Y. Molecular origin of the sawtooth behavior and the toughness of nacre. Mater Sci Eng, C. 2012;32:1542–7.

- 78. Li X, Xu ZH, Wang R. In situ observation of nanograin rotation and deformation in nacre. Nano Lett. 2006;6:2301–4.
- Li X, Chang WC, Chao YJ, Wang R, Chang M. Nanoscale structural and mechanical characterization of a natural nanocomposite material: the shell of red abalone. Nano Lett. 2004;4:613

 7.
- Podsiadlo P, Kaushik AK, Arruda EM, Waas AM, Shim BS, Xu J, et al. Ultrastrong and stiff layered polymer nanocomposites. Science. 2007;318:80–3.
- Munch E, Launey ME, Alsem DH, Saiz E, Tomsia AP, Ritchie RO. Tough, bio-inspired hybrid materials. Science. 2008;322:1516–20.
- 82. Xia S, Wang Z, Chen H, Fu W, Wang J, Li Z, et al. Nanoasperity: structure origin of nacre-inspired nanocomposites. ACS Nano. 2015;9:2167–72.
- 83. Grossman M, Bouville F, Erni F, Masania K, Libanori R, Studart AR. Mineral nano-interconnectivity stiffens and toughens nacre-like composite materials. Adv Mater. 2017;29:1605039.
- 84. Wang J, Cheng Q, Lin L, Jiang L. Synergistic toughening of bioinspired poly (vinyl alcohol)–clay–nanofibrillar cellulose artificial nacre. ACS Nano. 2014;8:2739–45.
- Mathiazhagan S, Anup S. Investigation of deformation mechanisms of staggered nanocomposites using molecular dynamics. Phys Lett A. 2016;380:2849–53.
- Singh PP, Ranganathan R. Tensile and viscoelastic behavior in nacre-inspired nanocomposites: a coarse-grained molecular dynamics study. Nanomaterials. 2022;12:3333.
- Beese AM, An Z, Sarkar S, Nathamgari SSP, Espinosa HD, Nguyen ST. Defect-tolerant nanocomposites through bioinspired stiffness modulation. Adv Funct Mater. 2014;24:2883– 91.
- Ruiz L, Xia W, Meng Z, Keten S. A coarse-grained model for the mechanical behavior of multi-layer graphene. Carbon. 2015;82:103–15.
- Xia W, Ruiz L, Pugno NM, Keten S. Critical length scales and strain localization govern the mechanical performance of multi-layer graphene assemblies. Nanoscale. 2016;8:6456–62.
- Liu N, Li S, Wang X. Mechanism of coupling polymer thickness and interfacial interactions on strength and toughness of noncovalent nacre-inspired graphene nanocomposites. Compos Sci Technol. 2023;241:110124.
- 91. Ghosh P, Katti DR, Katti KS. Mineral proximity influences mechanical response of proteins in biological mineral–protein hybrid systems. Biomacromolecules. 2007;8:851–6.
- Zhang N, Yang S, Xiong L, Hong Y, Chen Y. Nanoscale toughening mechanism of nacre tablet. J Mech Behav Biomed Mater. 2016;53:200–9.
- 93. Zhang X, Nguyen H, Daly M, Nguyen ST, Espinosa HD. Nanoscale toughening of ultrathin graphene oxide-polymer composites: mechanochemical insights into hydrogen-bonding/van der Waals interactions, polymer chain alignment, and steric parameters. Nanoscale. 2019;11:12305–16.
- 94. Soler-Crespo RA, Mao L, Wen J, Nguyen HT, Zhang X, Wei X, et al. Atomically thin polymer layer enhances toughness of graphene oxide monolayers. Matter. 2019;1:369–88.
- Singh PP, Ranganathan R. Superior protection conferred by multi-layered graphene-polyethylene nanocomposites under shock loading. ACS Appl Eng Mater. 2023;2:286-97.

96. Chaurasia A. Mulik RS. Parashar A. Polymer-based nanocomposites for impact loading: a review. Mech Adv Mater Struc. 2022;29:2581-606.

iournal

- 97. Chiang CC, Breslin J, Weeks S, Meng Z. Dynamic mechanical behaviors of nacre-inspired graphene-polymer nanocomposites depending on internal nanostructures. Extreme Mech Lett. 2021;49:101451.
- 98. Fu Y, Michopoulos J, Song JH. Dynamics response of polyethylene polymer nanocomposites to shock wave loading. J Polym Sci, Part B: Polym Phys. 2015;53:1292-302.
- 99. Elder RM, O'Connor TC, Chantawansri TL, Sliozberg YR, Sirk TW, Yeh IC, et al. Shock-wave propagation and reflection in semicrystalline polyethylene: a molecular-level investigation. Phys Rev Mater. 2017;1:043606.
- 100. Yang Z, Chiang CC, Meng Z. Investigation of dynamic impact responses of layered polymer-graphene nanocomposite films using coarse-grained molecular dynamics simulations. Carbon. 2023;203;202-10.
- 101. Chaurasia A, Jalan SK, Parashar A. An atomistic approach to study the dynamic and structural response in 2D nanofiller reinforced polyethylene nanocomposites under ultra-short shock pulse loading. Mech Mater. 2022;169:104305.
- 102. Cui J, Zeng F, Wei D, Wang Y. Unraveling the effects of geometrical parameters on dynamic impact responses of graphene reinforced polymer nanocomposites using coarse-grained molecular dynamics simulations. PCCP. 2024;26:19266-
- 103. Katti DR, Katti KS. Modeling microarchitecture and mechanical behavior of nacre using 3D finite element techniques. Part I Elastic properties. J Mater Sci. 2001;36:1411-7.
- 104. Katti D, Katti K, Sopp J, Sarikaya M. 3D finite element modeling of mechanical response in nacre-based hybrid nanocomposites. Comput Theor Polym Sci. 2001;11:397-404.
- 105. Katti DR, Pradhan SM, Katti KS. Modeling the organic-inorganic interfacial nanoasperities in a model bio-nanocomposite, nacre. Rev Adv Mater Sci. 2004;6:162-8.
- 106. Tang H, Barthelat F, Espinosa H. An elasto-viscoplastic interface model for investigating the constitutive behavior of nacre. J Mech Phys Solids. 2007;55:1410-38.
- 107. Bruet B, Qi H, Boyce M, Panas R, Tai K, Frick L, et al. Nanoscale morphology and indentation of individual nacre tablets from the gastropod mollusc Trochus niloticus. J Mater Res. 2005;20:2400-19.
- 108. Kearney C, Zhao Z, Bruet B, Radovitzky R, Boyce M, Ortiz C. Nanoscale anisotropic plastic deformation in single crystal aragonite. Phys Rev Lett. 2006;96:255505.
- 109. Askarinejad S, Rahbar N. Toughening mechanisms in bioinspired multilayered materials. J Roy Soc Interface. 2015;12:20140855.
- 110. Xu ZH, Yang Y, Huang Z, Li X. Elastic modulus of biopolymer matrix in nacre measured using coupled atomic force microscopy bending and inverse finite element techniques. Mater Sci Eng, C. 2011;31:1852-6.
- 111. Carvajal Loaiza MJ, Vallejo Ciro MI, Martinez RV. Finite element modeling and experimental validation of brickand-mortar structures with mesoscale interlocking interfaces. Finite Elements in Analysis and Design. 2025;249: 104370.

- 112. Xia H. Geng K. Pan H. Wang Z. Zhang Z. Wang B. A micromechanical model for bioinspired nanocomposites with interphase. Compos Struct. 2023;321:117316.
- 113. Budarapu P, Thakur S, Kumar S, Paggi M. Micromechanics of engineered interphases in nacre-like composite structures. Mechan Adv Mater Struct. 2021;28:2327-42.
- 114. Rao Y, Wan W, Wei N, Wang K. Frequency-dependent dynamic moduli prediction for general bio-inspired staggered platelet reinforced composites. Polym Compos. 2023;44:3268-80.
- 115. Maghsoudi-Ganjeh M, Lin L, Yang X, Zeng X. Computational modeling and simulation of bioinspired nacre-like composites. J Mater Res. 2021;36:2651-61.
- 116. Lee S, Lim DD, Pegg E, Gu GX. The origin of high-velocity impact response and damage mechanisms for bioinspired composites. Cell Rep Phys Sci. 2022;3.
- 117. Gu GX, Takaffoli M, Hsieh AJ, Buehler MJ. Biomimetic additive manufactured polymer composites for improved impact resistance. Extreme Mech Lett. 2016;9:317-23.
- 118. Li H, Geng K, Zhu B, Zhang Q, Wen Y, Zhang Z, et al. Mineral asperities reinforce nacre through interlocking and friction-like sliding. J Mech Phys Solids. 2024;190:105712.
- 119. Ji H, Liang S, Li Y, Li K, Yan Y, Li XW. Elucidating platelet interlocking strengthening and toughening mechanism of nacre: coupled effect of platelet size and shape. Available at SSRN 4925815.
- 120. Peng XL, Lee S, Wilmers J, Oh SH, Bargmann S. Orientationdependent micromechanical behavior of nacre: in situ TEM experiments and finite element simulations. Acta Biomater. 2022:147:120-8.
- 121. Grujicic M, Ramaswami S, Snipes J. Nacre-like ceramic/polymer laminated composite for use in body-armor applications. AIMS Mater Sci. 2015;3.
- 122. Knipprath C, Bond IP, Trask RS. Biologically inspired crack delocalization in a high strain-rate environment. J Roy Soc Interface. 2012;9:665-76.
- 123. Flores-Johnson E, Shen L, Guiamatsia I, Nguyen GD. A numerical study of bioinspired nacre-like composite plates under blast loading. Compos Struct. 2015;126:329-36.
- 124. Wei Z, Xu X. Gradient design of bio-inspired nacre-like composites for improved impact resistance. Comp Part B: Eng. 2021;215:108830.
- 125. Wu K, Song Y, Zhang X, Zhang S, Zheng Z, Gong X, et al. A prestressing strategy enabled synergistic energy-dissipation in impact-resistant nacre-like structures. Adv Sci. 2022;9: 2104867.
- 126. Patek SN, Korff W, Caldwell RL. Deadly strike mechanism of a mantis shrimp. Nature. 2004;428:819-20.
- 127. DeVries M, Murphy E, Patek S. Strike mechanics of an ambush predator: the spearing mantis shrimp. J Exp Biol. 2012;215:4374-84.
- 128. Steinhardt E, Hyun NP, Koh J, Freeburn G, Rosen MH, Temel FZ, et al. A physical model of mantis shrimp for exploring the dynamics of ultrafast systems. Proc Natl Acad Sci. 2021;118:e2026833118.
- 129. Weaver JC, Milliron GW, Miserez A, Evans-Lutterodt K, Herrera S, Gallana I, et al. The stomatopod dactyl club: a formidable damage-tolerant biological hammer. Science. 2012;336:1275-80.

- 130. Christensen TEK, Chua JQI, Wittig NK, Jørgensen MRV, Kantor I, Thomsen JS, et al. Flexible design in the stomatopod dactyl club. IUCrJ. 2023;10:288–96.
- 131. Delaunois Y, Tits A, Grossman Q, Smeets S, Malherbe C, Eppe G, et al. Design strategies of the mantis shrimp spike: how the crustacean cuticle became a remarkable biological harpoon. Nat Sci. 2023;3:e20220060.
- 132. Wu K, Song Z, Zhang S, Ni Y, Cai S, Gong X, et al. Discontinuous fibrous Bouligand architecture enabling formidable fracture resistance with crack orientation insensitivity. Proc Natl Acad Sci. 2020:117:15465–72.
- 133. Rivera J, Yaraghi NA, Huang W, Gray D, Kisailus D. Modulation of impact energy dissipation in biomimetic helicoidal composites. J Mater Res Technol. 2020;9:14619–29.
- 134. Rao Y, Xiong T, Yao S, Zhao H, Wang K. An analytical study on low velocity impact resistance behaviors of general bio-inspired helicoidal composite plates. Polym Compos. 2024;45:5227–43.
- Qin X, Marchi BC, Meng Z, Keten S. Impact resistance of nanocellulose films with bioinspired Bouligand microstructures. Nanoscale Adv. 2019;1:1351–61.
- 136. Caviness C, Chen Y, Yang Z, Wang H, Wu Y, Meng Z. Improved ballistic impact resistance of nanofibrillar cellulose films with discontinuous fibrous Bouligand architecture. J Appl Mech. 2024;91.
- 137. Natarajan B, Krishnamurthy A, Qin X, Emiroglu CD, Forster A, Foster EJ, et al. Binary cellulose nanocrystal blends for bioinspired damage tolerant photonic films. Adv Funct Mater. 2018;28:1800032.
- 138. Xiao K, Lei X, Chen Y, An Q, Hu D, Wang C, et al. Extraordinary impact resistance of carbon nanotube film with crosslinks under micro-ballistic impact. Carbon. 2021;175:478–89.
- 139. Li J, Zhao Y, Miao L, Hao W, Zhao G, Li J, et al. Bouligand-like structured CNT film with tunable impact performance through pitch angle and intertube interaction. Carbon. 2024;220: 118888
- 140. Garnica A, Aparicio E, Shishehbor M, Kisailus D, Bringa EM, Zavattieri PD. How crack twisting in Bouligand structures lead to damage delocalization and toughening. Extreme Mech Lett. 2024:71:102190.
- 141. Wu H, Guo A, Kong D, Wu J, Qu P, Wang S, et al. Preparation of Bouligand biomimetic ceramic composites and the effect of different fiber orientations on mechanical properties. J Manuf Processes. 2024;132:789–801.
- 142. Suksangpanya N, Yaraghi NA, Pipes RB, Kisailus D, Zavattieri P. Crack twisting and toughening strategies in Bouligand architectures. Int J Solids Struct. 2018;150:83–106.
- 143. Liu J, Lee H, Tan V. Failure mechanisms in bioinspired helicoidal laminates. Compos Sci Technol. 2018;157:99–106.
- 144. Tadayon M, Amini S, Wang Z, Miserez A. Biomechanical design of the mantis shrimp saddle: a biomineralized spring used for rapid raptorial strikes. IScience. 2018;8:271–82.
- 145. Abir M, Tay T, Lee H. On the improved ballistic performance of bio-inspired composites. Compos Part A. 2019;123:59–70.
- 146. Amini S, Tadayon M, Idapalapati S, Miserez A. The role of quasi-plasticity in the extreme contact damage tolerance of the stomatopod dactyl club. Nat Mater. 2015;14:943–50.
- 147. Jiang H, Ren Y, Liu Z, Zhang S, Lin Z. Low-velocity impact resistance behaviors of bio-inspired helicoidal composite lam-

- inates with non-linear rotation angle based layups. Compos Struct. 2019;214:463–75.
- Liu J, Lee H, Kong S, Tan V. Improving laminates through nonuniform inter-ply angles. Compos Part A. 2019;127:105625.
- 149. Mencattelli L, Pinho ST. Realising bio-inspired impact damagetolerant thin-ply CFRP Bouligand structures via promoting diffused sub-critical helicoidal damage. Compos Sci Technol. 2019;182:107684.
- Liu J, Singh A, Lee H, Tay T, Tan V. The response of bio-inspired helicoidal laminates to small projectile impact. Int J Impact Eng. 2020;142:103608.
- 151. Han Q, Shi S, Liu Z, Han Z, Niu S, Zhang J, et al. Study on impact resistance behaviors of a novel composite laminate with basalt fiber for helical-sinusoidal bionic structure of dactyl club of mantis shrimp. Compos Part B. 2020;191:107976.
- 152. Yang F, Xie W, Meng S. Global sensitivity analysis of low-velocity impact response of bio-inspired helicoidal laminates. Int J Mech Sci. 2020;187:106110.
- 153. Chua JQI, Srinivasan DV, Idapalapati S, Miserez A. Fracture toughness of the stomatopod dactyl club is enhanced by plastic dissipation: a fracture micromechanics study. Acta Biomater. 2021;126:339–49.
- 154. Yang J, Gu D, Lin K, Yuan L, Guo M, Zhang H, et al. Laser powder bed fusion of mechanically efficient helicoidal structure inspired by mantis shrimp. Int J Mech Sci. 2022;231:107573.
- 155. Yang X, Wang M, Bai P, Niu S, Song H, Ni J, et al. An ingenious composite microstructure of mantis shrimp appendage for improving impact resistance. Compos Sci Technol. 2023;244:110310.
- 156. Eltaher MA, Aleryani O, Melaibari A, Abdelrahman AA. Bending and vibration of a bio-inspired Bouligand composite plate using the finite-element method. Mech Compos Mater. 2024;59:1199–216.
- 157. Zhang J, Niu W, Li Y, Wu X, Guo Z, Luan Y. Mechanical performance and optimization strategies of mantis shrimp rod inspired beam structural composites. J Mater Res. 2024;39:1437–48.
- 158. Pro JW, Barthelat F. Is the Bouligand architecture tougher than regular cross-ply laminates? A discrete element method study. Extreme Mech Lett. 2020;41:101042.
- 159. Dong Z, Chen S, Gupta HS, Zhao X, Yang Y, Chang G, et al. In situ determination of the extreme damage resistance behavior in stomatopod dactyl club. Synchrotron Radiat. 2022;29:775–86.
- Yang F, Xie W, Meng S. Analysis and simulation of fracture behavior in naturally occurring Bouligand structures. Acta Biomater. 2021;135:473–82.
- Nie Y, Li D. A multiscale fracture model to reveal the toughening mechanism in bioinspired Bouligand structures. Acta Biomater. 2024;176:267–76.
- 162. Ko FK, Wan LY. Engineering properties of spider silk. In: Bunsell A, editors. Handbook of properties of textile and technical fibres. 2018:185–220.
- Vollrath F. Strength and structure of spiders' silks. Rev Mol Biotechnol. 2000;74:67–83.
- 164. Gosline JM, DeMont ME, Denny MW. The structure and properties of spider silk. Endeavour. 1986;10:37–43.
- 165. Patil SP, Kulkarni A, Markert B. Mechanical properties of dragline silk fiber using a bottom-up approach. J Compos Sc. 2022;6:95.

- 166. Xu M, Lewis RV. Structure of a protein superfiber: spider dragline silk. Proc Natl Acad Sci. 1990;87:7120–4.
- 167. Simmons AH, Michal CA, Jelinski LW. Molecular orientation and two-component nature of the crystalline fraction of spider dragline silk. Science. 1996;271:84–7.
- 168. Van Beek J, Hess S, Vollrath F, Meier B. The molecular structure of spider dragline silk: folding and orientation of the protein backbone. Proc Natl Acad Sci. 2002;99:10266–71.
- Exler JH, Hümmerich D, Scheibel T. The amphiphilic properties of spider silks are important for spinning. Angew Chem Int Ed. 2007;46:3559–62.
- 170. Liu Y, Shao Z, Vollrath F. Relationships between supercontraction and mechanical properties of spider silk. Nat Mater. 2005;4:901–5.
- 171. Emile O, Le Floch A, Vollrath F. Shape memory in spider draglines. Nature. 2006;440:621–1.
- 172. Keten S, Xu Z, Ihle B, Buehler MJ. Nanoconfinement controls stiffness, strength and mechanical toughness of β -sheet crystals in silk. Nat Mater. 2010;9:359–67.
- 173. Vendrely C, Scheibel T. Biotechnological production of spidersilk proteins enables new applications. Macromol Biosci. 2007:7:401–9.
- 174. Patel M, Dubey DK, Singh SP. Phenomenological models of *Bombyx mori* silk fibroin and their mechanical behavior using molecular dynamics simulations. Mater Sci Eng C. 2020;108:110414.
- 175. Pan L, Wang F, Cheng Y, Leow WR, Zhang YW, Wang M, et al. A supertough electro-tendon based on spider silk composites. Nat Commun. 2020:11:1332.
- 176. Amendola A, de Castro Motta J, Fraternali F. Discrete-to-continuum modeling of spider silk fiber composites. Int J Non Linear Mech. 2024;163:104735.
- 177. Venkatesan H, Chen J, Liu H, Kim Y, Na S, Liu W, et al. Artificial spider silk is smart like natural one: having humidity-sensitive shape memory with superior recovery stress. Mater Chem Front. 2019;3:2472–82.
- 178. Asakura T. Structure and dynamics of spider silk studied with solid-state nuclear magnetic resonance and molecular dynamics simulation. Molecules. 2020;25:2634.
- 179. Kim Y, Lee M, Baek I, Yoon T, Na S. Mechanically inferior constituents in spider silk result in mechanically superior fibres by adaptation to harsh hydration conditions: a molecular dynamics study. J Roy Soc Interface. 2018;15:20180305.
- 180. Rawal A, Rhinehardt KL, Mohan RV. Mechanical properties of spider silk for use as a biomaterial: molecular dynamics investigations. In: ASME International Mechanical Engineering Congress and Exposition. Vol. 84508. American Society of Mechanical Engineers; 2020.
- 181. Chang Z, Shen Y, Xue J, Sun Y, Zhang S. Fabrication of spider silk-inspired bio-based polymeric materials under dynamic nanoconfinement as high-strong, ultra-tough, and multifunctional plastic substitutes. Chem Eng J. 2023;457: 140984.
- 182. Momeni Bashusqeh S, Pugno N. Development of mechanically-consistent coarse-grained molecular dynamics model: case study of mechanics of spider silk. Sci Rep. 2023;13:19316.
- 183. Shin H, Yoon T, Park W, You J, Na S. Unraveling the mechanical property decrease of electrospun spider silk: a molecular

- dynamics simulation study. ACS Appl Bio Mater. 2024;7:1968–75
- 184. Zhao T, Ma H, Liu Y, Chen Z, Shi Q, Ning L. Interfacial interactions between spider silk protein and cellulose studied by molecular dynamics simulation. J Mol Model. 2024;30:156.
- 185. Yuan Z, Fang B, He Q, Wei H, Jian H, Zhang L. Molecular dynamics study of the structure and mechanical properties of spider silk proteins. Biomacromolecules. 2025.
- 186. Jiang Y, Nayeb-Hashemi H. Energy dissipation during prey capture process in spider orb webs. J Appl Mech. 2020;87:091009.
- Xu B, Yang Y, Zhang B, Yan Y, Yi Z. Bionic design and experimental study for the space flexible webs capture system. IEEE Access. 2020;8:45411–20.
- 188. Fraternali F, Stehling N, Amendola A, Tiban Anrango BA, Holland C, Rodenburg C. Tensegrity modelling and the high toughness of spider dragline silk. Nanomaterials. 2020;10:1510.
- Jiang Y, Nayeb-Hashemi H. A new constitutive model for dragline silk. Int J Solids Struct. 2020;202:99–110.
- 190. Kaewunruen S, Ngamkhanong C, Yang T. Large-amplitude vibrations of spider web structures. Appl Sci. 2020;10:6032.
- Kaewunruen S, Ngamkhanong C, Xu S. Large amplitude vibrations of imperfect spider web structures. Sci Rep. 2020;10: 19161.
- 192. Li G, Tian Q, Wu W, Yang S, Wu Q, Zhao Y, et al. Bioinspired 4D printing of dynamic spider silks. Polymers. 2022;14: 2069
- 193. Xie B, Wu X, Ji X. Investigation on the energy-absorbing properties of bionic spider web structure. Biomimetics. 2023;8:537.
- 194. Mohol SS, Kumar M, Sharma V. PLA-based nature-inspired architecture for bone scaffolds: a finite element analysis. Comput Biol Med. 2023;163:107163.
- 195. Rawat P, Liu S, Mahesh, Kumar R, Singh NK. Numerical investigation on the high-velocity impact resistance of textile reinforced composite mesh designs inspired by spider web. J Text Inst. 2024;115:1995–2010.
- 196. Boskey AL, Coleman R. Aging and bone. J Dent Res. 2010;89:1333–48.
- 197. Liu Y, Luo D, Wang T. Hierarchical structures of bone and bioinspired bone tissue engineering. Small. 2016;12:4611–32.
- 198. Rho JY, Kuhn-Spearing L, Zioupos P. Mechanical properties and the hierarchical structure of bone. Med Eng Phys. 1998;20:92–102.
- Fratzl P. Collagen: structure and mechanics, an introduction. In: Fratzl P, editors. Collagen: structure and mechanics. Springer; 2008. p. 1–13.
- 200. Li S, Demirci E, Silberschmidt VV. Variability and anisotropy of mechanical behavior of cortical bone in tension and compression. J Mech Behav Biomed Mater. 2013;21:109–20.
- 201. Goodyear SR, Gibson IR, Skakle JM, Wells RP, Aspden RM. A comparison of cortical and trabecular bone from C57 Black 6 mice using Raman spectroscopy. Bone. 2009;44:899–907.
- 202. Hench LL. Biomaterials: a forecast for the future. Biomaterials. 1998;19:1419–23.
- 203. Ammann P, Rizzoli R. Bone strength and its determinants. Osteop Int. 2003;14:13–8.
- 204. Nair AK, Gautieri A, Chang SW, Buehler MJ. Molecular mechanics of mineralized collagen fibrils in bone. Nat Commun. 2013;4:1724.

- 205. Bhowmik R, Katti KS, Katti DR, Mechanics of molecular collagen is influenced by hydroxyapatite in natural bone. J Mater Sci. 2007;42:8795-803.
- 206. Fielder M, Nair AK. Effects of hydration and mineralization on the deformation mechanisms of collagen fibrils in bone at the nanoscale. Biomech Model Mechanobiol. 2019;18:57-68.
- 207. Song Q, Jiao K, Tonggu L, Wang L, Zhang S, Yang Y, et al. Contribution of biomimetic collagen-ligand interaction to intrafibrillar mineralization. Sci Adv. 2019;5(3):eaav9075.
- 208. Milazzo M, Jung GS, Danti S, Buehler MJ. Mechanics of mineralized collagen fibrils upon transient loads. ACS Nano. 2020:14:8307-16.
- 209. Tavakol M, Vaughan TJ. A coarse-grained molecular dynamics investigation of the role of mineral arrangement on the mechanical properties of mineralized collagen fibrils. J Roy Soc Interface. 2023;20:20220803.
- 210. de Alcântara AC, Felix LC, Galvao DS, Sollero P, Skaf MS. The role of the extrafibrillar volume on the mechanical properties of molecular models of mineralized bone microfibrils. ACS Biomater Sci Eng. 2022;9:230-45.
- 211. Frank M, Marx D, Nedelkovski V, Pahr DH, Thurner PJ, et al. Dehydration of individual bovine trabeculae causes transition from ductile to quasi-brittle failure mode. J Mech Behav Biomed Mater. 2018;87:296-305.
- 212. Vercher-Martínez A, Giner E, Belda R, Aigoun A, Fuenmayor FJ. Explicit expressions for the estimation of the elastic constants of lamellar bone as a function of the volumetric mineral content using a multi-scale approach. Biomech Model Mechanobiol. 2018:17:449-64.
- 213. Wang Y, Ural A. Mineralized collagen fibril network spatial arrangement influences cortical bone fracture behavior. J Biomech. 2018;66:70-7.
- 214. Wang Y, Ural A. Effect of modifications in mineralized collagen fibril and extra-fibrillar matrix material properties on submicroscale mechanical behavior of cortical bone. J Mech Behav Biomed Mater. 2018;82:18-26.
- 215. Wang Y, Ural A. A finite element study evaluating the influence of mineralization distribution and content on the tensile mechanical response of mineralized collagen fibril networks. J Mech Behav Biomed Mater. 2019;100:103361.
- 216. Marco M, Giner E, Larraínzar-Garijo R, Caeiro JR, Miguélez MH. Modelling of femur fracture using finite element procedures. Eng Fract Mech. 2018;196:157-67.
- 217. Maghsoudi-Ganjeh M, Lin L, Wang X, Zeng X. Bioinspired design of hybrid composite materials. Int J Smart Nano Mater. 2019;10:90-105.
- 218. Maghsoudi-Ganjeh M, Lin L, Wang X, Wang X, Zeng X. Computational modeling of the mechanical behavior of 3D hybrid organic-inorganic nanocomposites. JOM. 2019;71: 3951-61.
- 219. Maghsoudi-Ganjeh M, Wang X, Zeng X. Computational investigation of the effect of water on the nanomechanical behavior of bone. J Mech Behav Biomed Mater. 2020;101:103454.
- 220. Nikkhah H, Baroutaji A, Kazancı Z, Arjunan A. Evaluation of crushing and energy absorption characteristics of bio-inspired nested structures. Thin-Wall Struct. 2020;148:106615.
- 221. Wang C, Li Y, Zhao W, Zou S, Zhou G, Wang Y. Structure design and multi-objective optimization of a novel crash box based on biomimetic structure. Int J Mech Sci. 2018;138:489-501.

- 222. Salem M. Westover L. Adeeb S. Duke K. An equivalent constitutive model of cancellous bone with fracture prediction. J Biomech Eng. 2020;142:121004.
- 223. Belda R, Palomar M, Peris-Serra JL, Vercher-Martínez A, Giner E. Compression failure characterization of cancellous bone combining experimental testing, digital image correlation and finite element modeling. Int J Mech Sci. 2020;165:105213.
- 224. Demirtas A, Ural A. Interaction of microcracks and tissue compositional heterogeneity in determining fracture resistance of human cortical bone. J Biomech Eng. 2018;140:091003.
- 225. Marco M. Belda R. Miguélez MH. Giner E. A heterogeneous orientation criterion for crack modelling in cortical bone using a phantom-node approach. Finite Elem Anal Des. 2018;146:107-17.
- 226. Gustafsson A, Wallin M, Khayyeri H, Isaksson H. Crack propagation in cortical bone is affected by the characteristics of the cement line: a parameter study using an XFEM interface damage model. Biomech Model Mechanobiol. 2019;18:1247-61.
- 227. Gustafsson A, Khayyeri H, Wallin M, Isaksson H. An interface damage model that captures crack propagation at the microscale in cortical bone using XFEM. J Mech Behav Biomed Mater. 2019:90:556-65.
- 228. Razi H, Predan J, Fischer FD, Kolednik O, Fratzl P. Damage tolerance of lamellar bone. Bone. 2020;130:115102.
- 229. Choudhary K, DeCost B, Chen C, Jain A, Tavazza F, Cohn R, et al. Recent advances and applications of deep learning methods in materials science. npj Comput Mater. 2022;8:59.
- 230. Magsood A, Chen C, Jacobsson TJ. The future of material scientists in an age of artificial intelligence. Adv Sci. 2024;11:2401401.
- 231. Curtarolo S, Setyawan W, Hart GL, Jahnatek M, Chepulskii RV, Taylor RH, et al. AFLOW: an automatic framework for high-throughput materials discovery. Comput Mater Sci. 2012;58:218-26.
- 232. Esters M, Oses C, Divilov S, Eckert H, Friedrich R, Hicks D, et al. aflow. org: a web ecosystem of databases, software and tools. Comput Mater Sci. 2023;216:111808.
- 233. Jain A, Ong SP, Hautier G, Chen W, Richards WD, Dacek S, et al. Commentary: The Materials Project: a materials genome approach to accelerating materials innovation. APL Mater. 2013;1(1).
- 234. Jain A, Montoya J, Dwaraknath S, Zimmermann NE, Dagdelen J, Horton M, et al. The Materials Project: accelerating materials design through theory-driven data and tools. In: Andreoni W, Yip S, editors. Handbook of materials modeling: methods: theory and modeling. 2020:1751-84.
- 235. Spotte-Smith EWC, Cohen OA, Blau SM, Munro JM, Yang R, Guha RD, et al. A database of molecular properties integrated in the Materials Project. Digit Discov. 2023;2:1862-82.
- 236. Hellenbrandt M. The inorganic crystal structure database (ICSD)-present and future. Crystallogr Rev. 2004;10:17-22.
- 237. Saal JE, Kirklin S, Aykol M, Meredig B, Wolverton C. Materials design and discovery with high-throughput density functional theory: the Open Quantum Materials Database (OQMD). JOM. 2013;65:1501-9.
- 238. Shen J, Griesemer SD, Gopakumar A, Baldassarri B, Saal JE, Aykol M, et al. Reflections on one million compounds in the Open Quantum Materials Database (OQMD). J Phys Mater. 2022;5:031001.

239. Choudhary K. Garrity KF. Reid AC. DeCost B. Biacchi AJ. Hight Walker AR, et al. The Joint Automated Repository for Various Integrated Simulations (JARVIS) for data-driven materials design. npj Comput Mater. 2020;6:173.

journal

- 240. Wines D, Gurunathan R, Garrity KF, DeCost B, Biacchi AJ, Tavazza F, et al. Recent progress in the JARVIS infrastructure for next-generation data-driven materials design. Appl Phys Rev. 2023:10(4).
- 241. Draxl C, Scheffler M. NOMAD: the FAIR concept for big datadriven materials science. MRS Bullet. 2018;43:676-82.
- 242. Draxl C. Scheffler M. Big data-driven materials science and its FAIR data infrastructure. In: Andreoni W, Yip S, editors. Handbook of materials modeling: methods: theory and modeling. Springer; 2020. p. 49-
- 243. Borysov SS, Geilhufe RM, Balatsky AV. Organic Materials Database: an open-access online database for data mining. PLoS One. 2017;12(2):e0171501.
- 244. Gu GX, Chen CT, Richmond DJ, Buehler MJ. Bioinspired hierarchical composite design using machine learning: simulation, additive manufacturing, and experiment. Mater Horiz. 2018:5:939-45.
- 245. Chen CT, Gu GX. Effect of constituent materials on composite performance: exploring design strategies via machine learning. Adv Theor Simul. 2019;2:1900056.
- 246. Gu GX, Chen CT, Buehler MJ. De novo composite design based on machine learning algorithm. Extreme Mech Lett. 2018;18:19-28.
- 247. Al-Maskari N, McAdams DA, Reddy JN. Modeling of a biological material nacre: multi-objective optimization model. Mechan Adv Mater Struct. 2021;28:430-9.
- 248. Zhang X, Ding B, Cheng R, Dixon SC, Lu Y. Computational intelligence-assisted understanding of nature-inspired superhydrophobic behavior. Adv Sci. 2018;5:1700520.
- 249. Morsali S, Qian D, Minary-Jolandan M. Designing bioinspired brick-and-mortar composites using learning and statistical learning. Commun Mater. 2020;1:
- 250. Sarvestani HY, Singh A, Ashrafi B. Bridging nature and technology: a perspective on role of machine learning in bioinspired ceramics. Adv Eng Mater. 2024:2400792.
- 251. Shen SC, Buehler MJ. Nature-inspired architected materials using unsupervised deep learning. Comm Eng. 2022;1:37.
- 252. Mao Y, He Q, Zhao X. Designing complex architectured materials with generative adversarial networks. Sci Adv. 2020;6(17):eaaz4169.

- 253. Siegkas P. Generating 3D porous structures using machine learning and additive manufacturing. Mater Des. 2022;220:110858.
- 254. Badini S, Regondi S, Pugliese R. Enhancing mechanical and bioinspired materials through generative AI approaches. Next Mater. 2025;6:100275.
- 255. Wang XQ, Jin Z, Ravichandran D, Gu GX. Artificial intelligence and multiscale modeling for sustainable biopolymers and bioinspired materials. Adv Mater. 2025;37:2416901.
- 256. Yang Y, Song X, Li X, Chen Z, Zhou C, Zhou Q, et al. Recent progress in biomimetic additive manufacturing technology: from materials to functional structures. Adv Mater. 2018;30:1706539.
- 257. Wu H, Guo A, Kong D, Li X, Wu J, Wang H, et al. Nacre-like carbon fiber-reinforced biomimetic ceramic composites: fabrication, microstructure, and mechanical performance. Ceram Int. 2024;50:25388-99.
- 258. Chen S, Zhou Y, Xiao S, Zheng Y, Chen W, Li W, et al. An experimental and theoretical study of biomimetic cementepoxy resin composites: structure, mechanical properties, and reinforcement mechanisms. Compos Part A. 2024;185:108297.
- 259. Song K, Liu J, Dong J, Liang Y, Du T, Fan H, et al. Tailorable nanoconfinement enables nacreous biomimetic graphene/silicate composites with ultrahigh strength and toughness. Carbon. 2025;240:120364.
- 260. Song K, Yang S, Wei Y, Shao N, He P, Zhao Y, et al. Coaxially printed biomimetic BSPC with high strength and toughness. Mater Des. 2024;238:112648.
- 261. Yu C, Wang M, Zhang D, Liang K, Zhou M, Fu J, et al. Musselinspired robust and waterproof soybean protein adhesives enhanced with phenolated lignosulfonate for wood bonding. Int J Biol Macromol. 2025;314:144419.
- 262. Sun J, Yu S, Wade-Zhu J, Wang Y, Qu H, Zhao S, et al. 3D printing of ceramic composite with biomimetic toughening design. Addit Manuf. 2022;58:103027.

How to cite this article: Upadhyay SD, Singh PP, Thakur V, Ranganathan R. Recent advances in modeling structure-property relations in biomimetic materials at the molecular and continuum scales. J Am Ceram Soc. 2025;e70241. https://doi.org/10.1111/jace.70241